Supplementary information for:

Global exposure and vulnerability to multi-sector development and climate change hotspots

Edward Byers[1], Matthew Gidden[1], David Leclère[1], Peter Burek[1], Kristie Ebi[2], Peter Greve[1], David Grey[3], Petr Havlik[1], Astrid Hillers[4], Nils Johnson[1], Taher Kahil[1], Volker Krey[1], Simon Langan[1], Nebjosa Nakicenovic[1], Robert Novak[5], Michael Obersteiner[1], Shonali Pachauri[1], Amanda Palazzo[1], Simon Parkinson[1], Narasimha Rao[1], Joeri Rogelj[1], Yusuke Satoh[1], Yoshihide Wada[1], Barbara Willaarts[1], Keywan Riahi[1]

[1] International Institute for Applied Systems Analysis, Schlossplatz 1, 2362 Laxenburg, Austria
[2] University of Washington, Center for Health and Global Environment, Box 354695, Seattle, WA 98105, United States
[3] University of Oxford, School of Geography and the Environment, Oxford, OX1 3QY, United Kingdom
[4] Global Environment Facility, 1818 H Street NW, Washington, DC 20433, United States
[5] United National Industrial Development Organization, Wagramer Str. 5, 1220 Vienna, Austria

Table of Contents

1. Additional indicator and methodological information

1.1. GCM year selection for the temperature timeslices at 1.5°C, 2.0°C and 3.0°C

As in previous assessments, 30-year timeslices are selected by centering the timeslice over the year at which the GCM global mean temperature passes the desired temperature threshold. This is possible because previous work empirically found that GMT change is largely independent of the speed of the emissions pathway [1, 2], known as the 'transient climate response to emissions' [3, 4].

In most cases, we use data from RCP8.5 such that all five GCMs pass 3.0°C by 2085. In some indicators, where the SSP-RCP combination is endogenous to the model, RCP4.5 and RCP6.0 were used, thus the number of 3.0° scenarios is limited to GCMs that hit 3.0°C by 2085 (see SI Table S2 for exact model/RCP details).

Table S 1. 30-year periods selected for each global mean temperature level above pre-industrial conditions for the different GCMs.

RCP8.5 30yr periods	**Historical baseline (~0.6°C)**	**1.5°C**	**2.0°C**	**3.0°C**
GFDL-ESM2M	1971-2000	2019-2048	2036-2065	2066-2095
HadGEM2-ES	1971-2000	2002-2031	2014-2043	2035-2064
IPSL-CM5A-LR	1971-2000	2007-2036	2019-2048	2039-2068
MIROC-ESM-CHEM	1971-2000	2004-2033	2016-2045	2035-2064
NorESM1-M	1971-2000	2014-2043	2030-2059	2056-2085

RCP6.0 30yr periods	**Historical baseline**	**1.5°C**	**2.0°C**	**3.0°C**
GFDL-ESM2M	1971-2000	2036-2064	2058-2087	-
HadGEM2-ES	1971-2000	2005-2034	2023-2052	2053-2082
IPSL-CM5A-LR	1971-2000	2010-2039	2029-2058	2067-2096
MIROC-ESM-CHEM	1971-2000	2009-2038	2025-2054	2053-2082
NorESM1-M	1971-2000	2028-2057	2051-2080	-

RCP4.5 30yr periods	**Historical baseline**	**1.5°C**	**2.0°C**	**3.0°C**
GFDL-ESM2M	1971-2000	2027-2056	-	-
HadGEM2-ES	1971-2000	2005-2034	2021-2052	2053-2082
IPSL-CM5A-LR	1971-2000	2009-2038	2025-2054	-
MIROC-ESM-CHEM	1971-2000	2008-2037	2021-2050	2056-2085
NorESM1-M	1971-2000	2018-2047	2048-2077	-

1.2. Additional methodological description justification for year 2050.

The year 2050 was chosen to make meaningful and consistent comparison between SSP socioeconomic projections. In this year, the three levels of GMT change (1.5°C, 2.0°C and 3.0°C) can be achieved with varying probability, due to the range of scenarios and geophysical response uncertainty[5, 6]. This was verified for consistency using the IPCC Working Group III scenario database (available online at: https://secure.iiasa.ac.at/web-apps/ene/AR5DB/)[7].

We illustrate this consistency with the temperature projection data and its associated uncertainties from the IPCC Working Group III scenario database. Median temperature projections for the year 2050 range from 1.5°C to 2.26°C across the range of more than 300 scenarios. Furthermore, because of uncertainties in the carbon-cycle and climate response, these projections are accompanied by an uncertainty range; the 95th percentile of temperature projections of the same set of scenarios shows that warming can also reach 3°C by 2050, albeit with lower likelihood. In about 20% of scenarios, warming at the 95th percentile exceeds 3°C in 2050. This thus illustrates that the three GMT levels used in this study are within the range of scenario and geophysical response uncertainty assessed for the year 2050. [5, 6].

1.3. Indicator and model information

Additional details on the indicators is found in Table S 2. Below, maps of each indicator are presented.

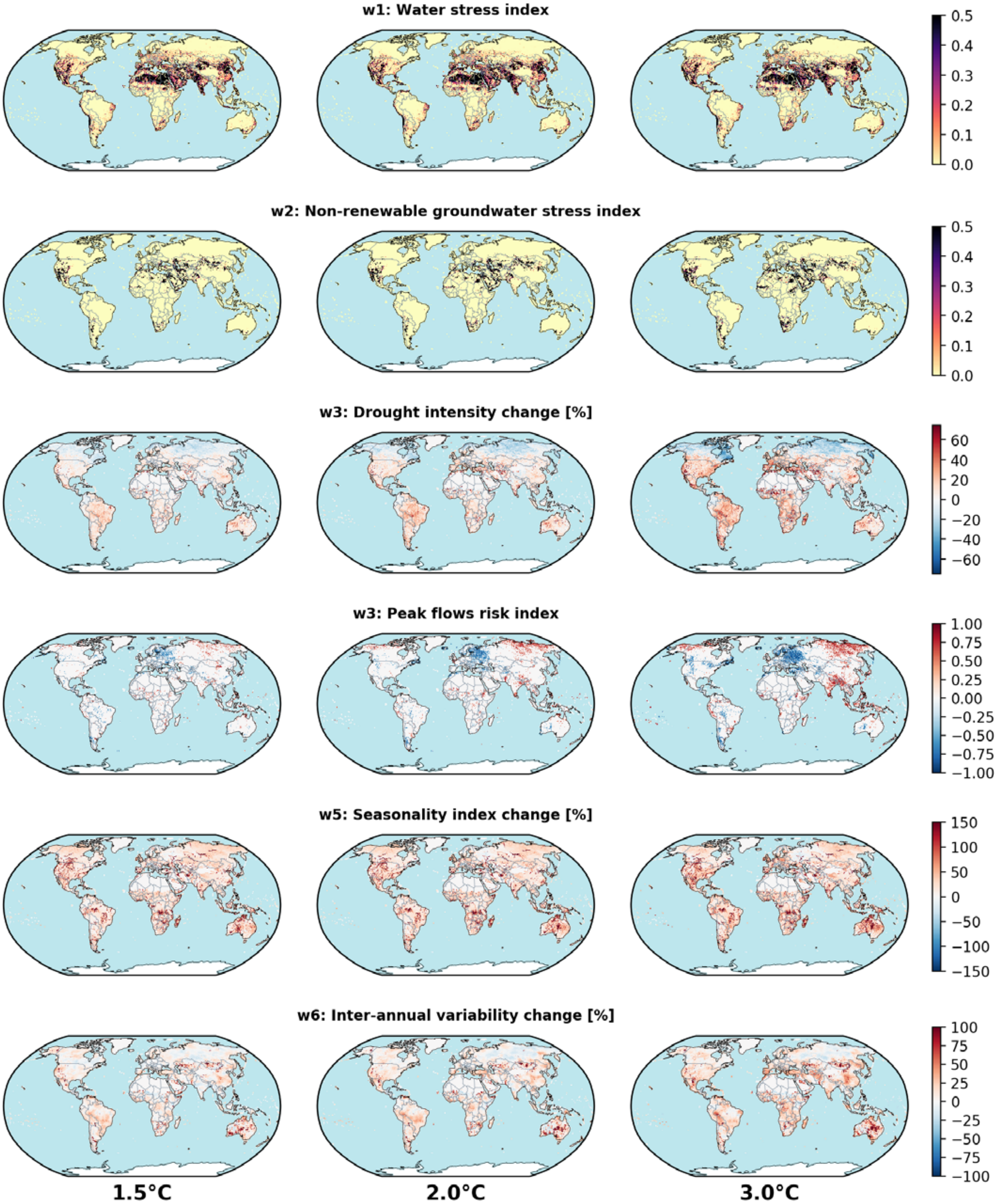

Figure S 1. Water indicators for 1.5, 2.0 and 3.0°C GMT change.

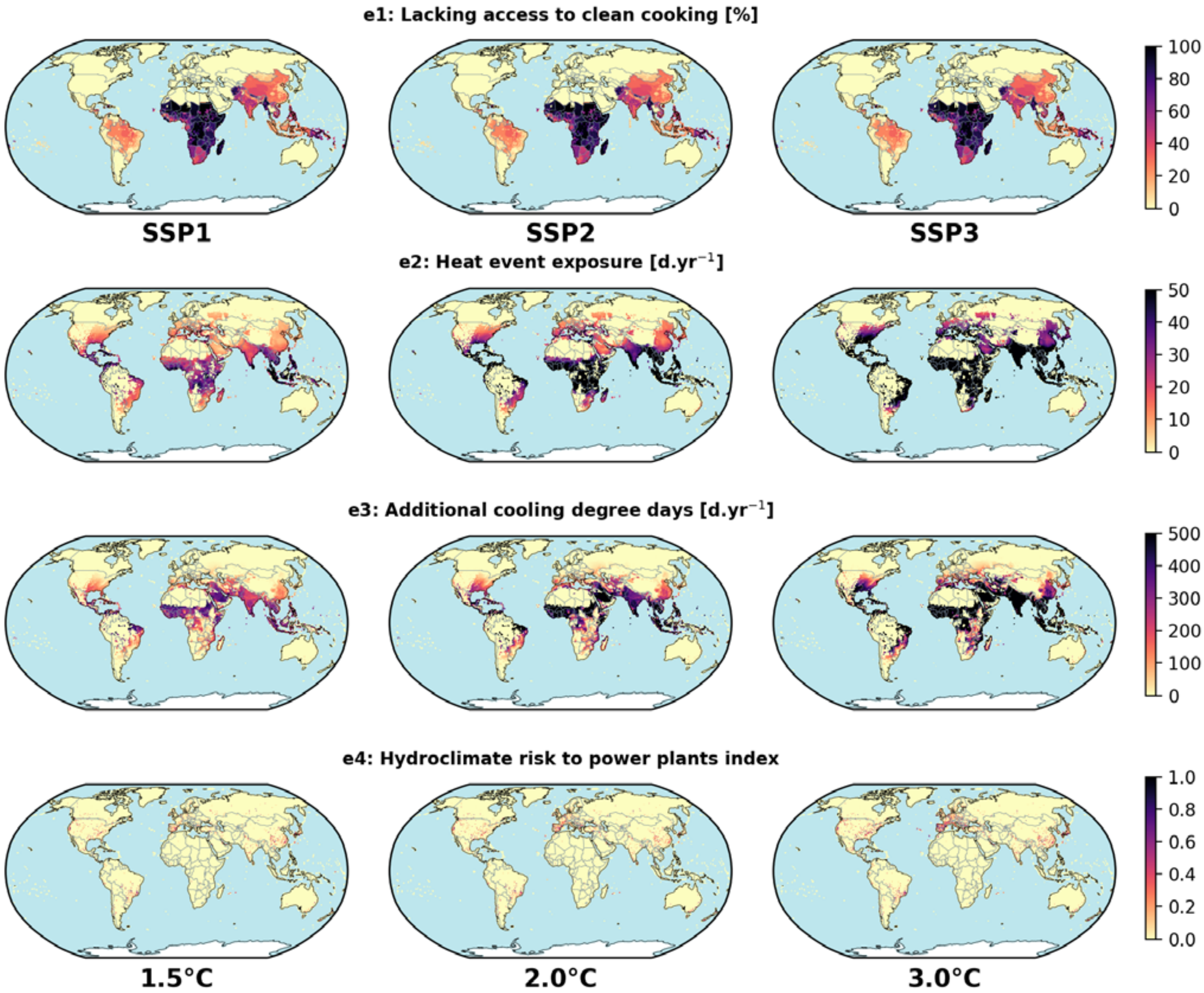

Figure S 2. Energy indicators. Clean cooking for SSP1, SSP2 and SSP3. Others are for 1.5, 2.0 and 3.0°C GMT change.

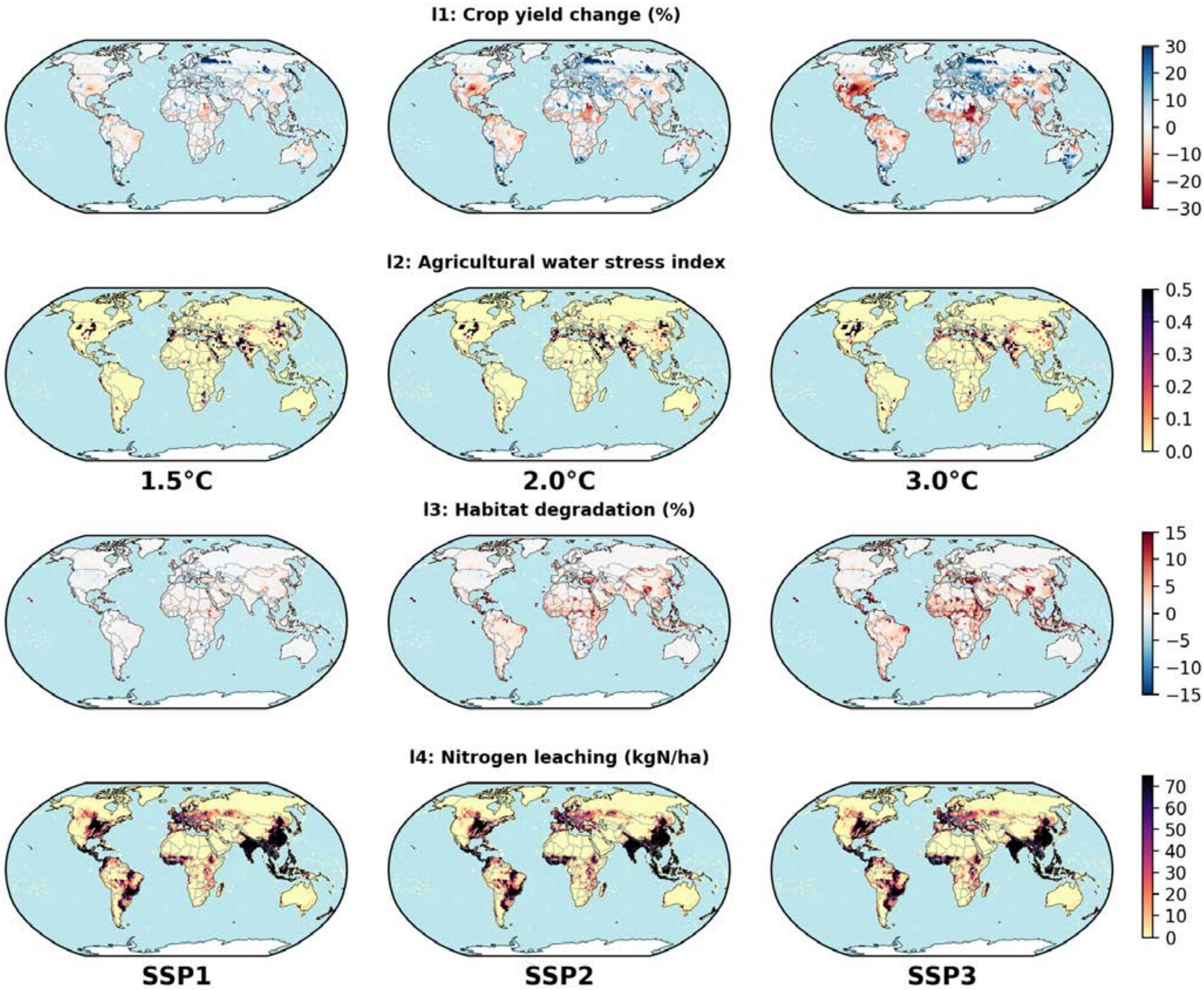

Figure S 3. Land indicators. Crop yield and Agricultural water stress index presented for 1.5, 2.0 and 3.0°C GMT change. Habitat degradation and Nitrate leaching presented for SSP1, SSP2 and SSP3.

Table S 2. Detailed indicator information.

indicator	name	description	Models & data
w1	Water stress index	Water stress index: as a fraction of net human demands (domestic, industrial, irrigation) divided by renewable surface water availability, as known as the withdrawal to availability ratio [8]. The index was calculated using ISIMIP Fast Track data from PCRGLOBWB, WaterGAP and H08 hydrological models using monthly discharge data (with societal discharge routing "pressoc"). Water demands were calculated using the SSPs from the IIASA Water Futures and Solutions initiative where more details of the scenario development and model descriptions can be found [9, 10].	GCMs: 5 x ISIMIP GCMs RCP8.5 Hydrology: PCRGLOBWB; WaterGAP; H08
w2	Non-renewable GW abstraction index	Non-renewable groundwater stress index (w2) is calculated as the fraction of total groundwater abstraction that is non-renewable using data from Wada and Bierkens [11], [12]. The transient assessment spanned 1960-2099 to thus compare historical and projected groundwater abstractions.	GCM: HadGEM2-ES RCP6.0 Hydrology: PCRGLOBWB
w3	Drought intensity	Change in drought intensity (w3) is calculated and the proportion between daily water volume deficit (m^3/s) below the 10^{th} percentile daily discharge (Q_{90}) and drought event duration (days), as derived in Wanders and Wada [13].	GCMs: 5 x ISIMIP GCMs RCP8.5 Hydrology: H.08; LPJmL; PCRGLOBWB; MPI-HM; WBM+
w4	Peak flows risk	Peak flows risk (w4) is derived using a block-maxima approach with Generalized Extreme Value distribution fitting as in Dankers, Arnell [14] to produce return period values for both historical and future hydrological simulations. With a 20-member ensemble, only locations where there is significant (50%+) ensemble agreement of a doubling or halving of the 20-year return period for river discharge were retained.	GCMs: 5 x ISIMIP GCMs RCP8.5 Hydrology: H.08; LPJmL; PCRGLOBWB; WBM+
w5	Seasonality	Mean seasonality (w5) is the change in seasonality index, calculated as the coefficient of variation (standard deviation divided by the mean) of mean monthly discharge. Lower values (<1) represent low seasonality (i.e. flows do not vary much through the year).	GCMs: 5 x ISIMIP GCMs RCP8.5 Hydrology: H.08; LPJmL; PCRGLOBWB; MPI-HM; WBM+
w6	Inter-annual variability	Mean inter-annual variability (w6), is the change in inter-annual variability index, calculated as the coefficient of variation (standard deviation divided by the mean) of mean annual discharge. Lower values represent (<0.5) low inter-annual variability (i.e. annual flows do not vary much between years).	GCMs: 5 x ISIMIP GCMs RCP8.5 Hydrology: H.08; LPJmL; PCRGLOBWB; MPI-HM; WBM+
e1	Access to clean cooking	Access to clean cooking (e1) is projected from the reference energy scenarios for each SSP on a regional basis (IIASA-SSP database). Results for cooking energy access under a no policy scenario developed for the Global Energy Assessment are used to estimate the elasticity of change in access with respect to income [15, 16] .The regional elasticity of access to income estimates are then applied to determine regional access under each SSP scenario, considering differences in incomes across these. Assuming that it is the poorest that do not have access to clean cooking, this fraction is used to calculate the income threshold for combination of region, year and SSP and locate the population using the gridded income data [17]. Whilst ideally this could include feedbacks with GLOBIOM to understand forest degradation, it is worth noting however, that in several parts of the world, the sources of biomass used for cooking is not forests, but rather crops, animal residue and fallen twigs and branches on common lands and from private field borders etc. In parts of sub-Saharan Africa where charcoal use for cooking is very high, there is indeed a link between charcoal demand and forest degradation and deforestation, but this is not the case in much of Asia or Latin America [18].	MESSAGE for SSPs1-3 Gridded population and income levels aggregated from 0.125 to 0.5°.
e2	Heat event exposure	Change in heat event exposure (e2) is calculated as the sum of days from heat events lasting 3 or more consecutive days above the historical 99th percentile daily mean wet bulb air temperature. Values are then annualised over the 30-year period. Heat event are intended to represent impacts, not only to human health, but also on the energy sector, for which it is know that energy demand can spike, capacity of gas turbines decreases, reliability and efficiency of grid transmission infrastructure reduces. [19, 20]	GCMs: 5 x ISIMIP GCMs RCP8.5

e3	Cooling demand growth	Cooling demand growth (e3) is based on the absolute change in cooling degree days above a 26°C set-point temperature for the daily mean air temperature.	GCMs: 5 x ISIMIP GCMs RCP8.5
e4	Hydroclimate risk to power production	Hydroclimate risk to power production (e4) aggregates the combined hazard of four hydrological indicators (as used in this study), peak flows risk, drought intensity change, seasonality and inter-annual variability to a continuous risk scale (as used with other indicators). This is multiplied by a capacity score according to the installed capacity in each gridsquare, using a global dataset of water-dependent thermal and hydro power plant capacity [21-23]. The product of these two scores (hazard x exposure) gives the hydroclimate risk to power plants.	GCMs: 5 x ISIMIP GCMs RCP8.5 Hydrology: H.08; LPJmL; PCRGLOBWB; MPI-HM; WBM+ Power plants: World Electric Power Plant Database, CARMA power plant database; Additional information by Catherine Raptis.
l1	Crop yield change	Climate change impact on crop yield (l1) is estimated by the EPIC crop model under for ISIMIP future climate change scenarios [24] for 18 crops and 4 crop managements systems and overlaid with the distribution of crops and systems as estimated by the GLOBIOM land use model [25] for year 2000 [26] before being aggregated across crops and crop management pixels (using calorie content).	Land model: GLOBIOM + EPIC GCMs: 5 x ISIMIP GCMs RCP8.5 Hydrology: LPJmL
l2	Agricultural water exploitation index	Agricultural water stress index (l2) indicates agriculturally-driven environmental water stress. By identifying locations where the monthly irrigated water demand are in excess of sustainable supply, it measures the fraction of environmental flow requirement (EFR) agricultural demand required to meet the agricultural demands [27-29].	Land model: GLOBIOM GCM: HadGEM2-ES RCP8.5 Hydrology: LPJmL
l3	Habitat degradation	Habitat degradation (l3) is estimated as a % change from the share of land area within a pixel being converted from natural land to agricultural land (cropland and grassland) in the future as simulated by the GLOBIOM model [25, 30] and further downscaled to 0.5° [31]	Land model: GLOBIOM + downscaling GCM: HadGEM2-ES RCP4.5, 6.0
L4	Nitrogen balance/leaching	Nitrate leaching from mineral fertilizer application over cropland (l4) is the flux of nitrate resulting from mineral fertilizer application to cropland and lost to surface water streams as simulated by EPIC [32] for current conditions for 18 crops and crop management systems, and overlaid with GLOBIOM assumptions on R&D-induced future changes in crop yield and crop input use efficiency [33, 34] and downscaled GLOBIOM projections of the distribution of crop and crop management systems.	Land models: GLOBIOM + EPIC + downscaling GCM: HadGEM2-ES RCP4.5, 6.0

1. 5 x ISIMIP GCMs are: GFDL-ESM2M HadGEM2-ES, IPSL-CM5A-LR, MIROC-ESM-CHEM, NorESM1-M
2. All gridded models at 0.5° resolution unless otherwise stated.
3. In all cases using multiple model ensembles, the model median is used.

Table S 3. Model references and further information

Model name	Type	Institution*	References
GFDL-ESM2M	General Circulation Model	National Oceanic and Atmospheric Administration, US	[35]
HadGEM2-ES	General Circulation Model	Hadley Centre, Met Office, UK	[36]
IPSL-CM5A-LR	General Circulation Model	Institut Pierre Simon Laplace, France	[37]
MIROC-ESM-CHEM	General Circulation Model	Japan Agency for Marine-Earth Science and Technology, Japan	[38]
NorESM1-M	General Circulation Model	UNI Bjerknes Centre for Climate Research, Norway	[39]
H.08	Gridded global hydrological model	National Institute for Environmental Studies, Japan	[40]
LPJmL	Dynamic Global Vegetation model	Potsdam Institute for Climate Impact Research, Germany	[41]
PCRGLOBWB	Gridded global hydrological model	University of Utrecht, Netherlands	[42, 43]
MPI-HM	Gridded global hydrological model	Max Planck Institute for Meteorology, Germany	[44]
WBM+	Gridded global hydrological model	City University of New York, US	[45]
EPIC	Land management impacts model	International Institute for Applied Systems Analysis, Austria	[32]
GLOBIOM	Agro-economic crop and land-use model	International Institute for Applied Systems Analysis, Austria	[25, 30]
MESSAGE	Integrated Assessment energy-economic model	International Institute for Applied Systems Analysis, Austria	[30, 46, 47]
Salamanca	Gridded income and inequality model	International Institute for Applied Systems Analysis, Austria	[17]

* From which the relevant model runs are derived, not necessarily original host/ creator of the model.

1.4. Indicator scoring schematic example

i. In the top right panel, the original dataset, in this case w3 Drought Intensity (% change) is shown, with varying degrees of drought intensity change expected across the world.

ii. In the top left panel, the changes (increasing intensity) are shown with the dotted arrows depicting the ranges selected by the modelling teams for each intermediate risk category on the scale.

iii. In the bottom left panel, the mapping from original indicator value (x-axis) is made to indicator score (y-axis). The grey lines show the randomly and uniformly sampled points, 100 for each of the 4 ranges, that sample the low-high range of the expert judgement. For example, high impact in drought intensity change in Figure S 4 are considered between 60-80% change. The red line shows the median points of the range. This uncertainty is carried through and displayed in the distribution functions of Figure 3 of the main text.

iv. In the bottom right, every pixel of the indicator is converted to a score between 0 and 3, using the score function (either the median case or one of the random samples in the case of running the uncertainty analysis).

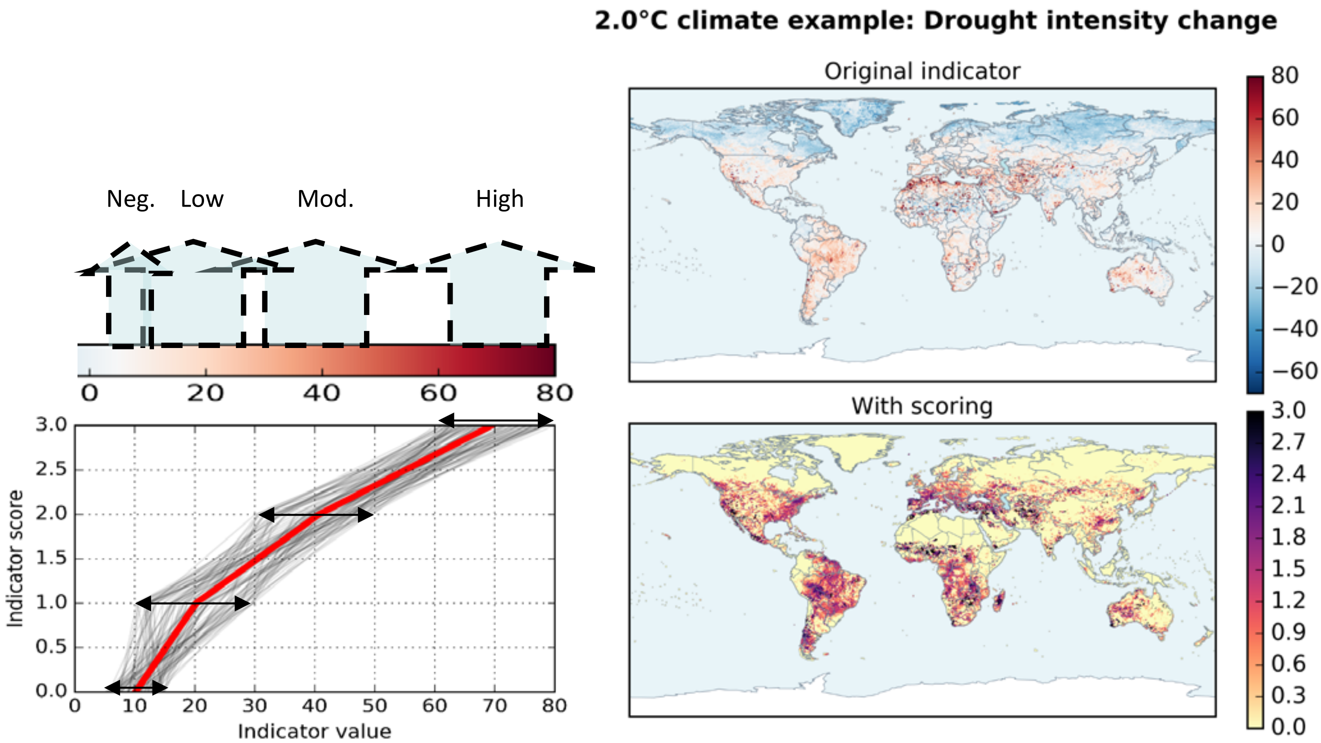

Figure S 4. Schematic showing the conversion of an indicator map (top right) into an indicator score map (bottom right) using the values from Table S 4. Described in more detail (i to iv) above.

1.5. Indicator score ranges

Table S 4. Table of indicators showing the weights, type of scale and low, central and high ranges selected for the analysis. Where scale is "index", the data is constrained between 0-1. Where scale is "relative", the data is expressed as a percentage change (%).

				CENTRAL				CONSERVATIVE (HIGH VALUES)				PRECAUTIONARY (LOW VALUES)			
Indicator	**Name**	**Scale**	**Weights**	**3**	**2**	**1**	**0**	**3**	**2**	**1**	**0**	**3**	**2**	**1**	**0**
w1	Water stress index	Index	1	0.4	0.3	0.2	0.1	0.5	0.4	0.25	0.15	0.3	0.2	0.1	0.05
w2	Non-renewable GW abstraction index	Index	1	0.4	0.3	0.2	0.1	0.5	0.4	0.25	0.15	0.3	0.2	0.1	0.05
w3	Drought intensity change	Relative	1	70	40	20	10	80	50	30	15	60	30	10	5
w4	Peak flows risk index	Index	1	0.75	0.65	0.55	0.49	0.85	0.6	0.5	0.49	0.65	0.55	0.5	0.49
w5	Seasonality index change	Relative	1	150	50	20	10	200	100	45	20	100	50	20	10
w6	Inter-annual variability index change	Relative	1	100	50	20	10	150	50	20	10	100	40	15	10
e1	Lack of access to clean cooking	Index	1	0.6	0.4	0.1	0.02	0.8	0.5	0.2	0.05	0.5	0.3	0.08	0.01
e2	Heat event exposure	Absolute	1	50	20	8	4	75	25	10	5	30	15	6	3
e3	Cooling demand growth	Absolute	1	400	250	100	20	500	325	150	30	300	200	75	10
e4	Hydroclimate risk to power index	Index	1	0.5	0.35	0.1	0.01	0.6	0.5	0.2	0.05	0.4	0.27	0.08	0.01
l1	Crop yield change	Relative	1	-15	-10	-5	-3	-20	-15	-7	-4	-10	-7	-3	-2
l2	Agricultural water stress index	Index	1	0.4	0.2	0.1	0.05	0.5	0.3	0.2	0.15	0.3	0.15	0.08	0.03
l3	Habitat degradation	Relative	1	10	8	3	1	12	10	4	1	8	6	2	0.5
l4	Nitrogen leaching	Absolute	1	75	50	20	5	100	70	30	10	50	30	10	3

1.6. Indicator score plots

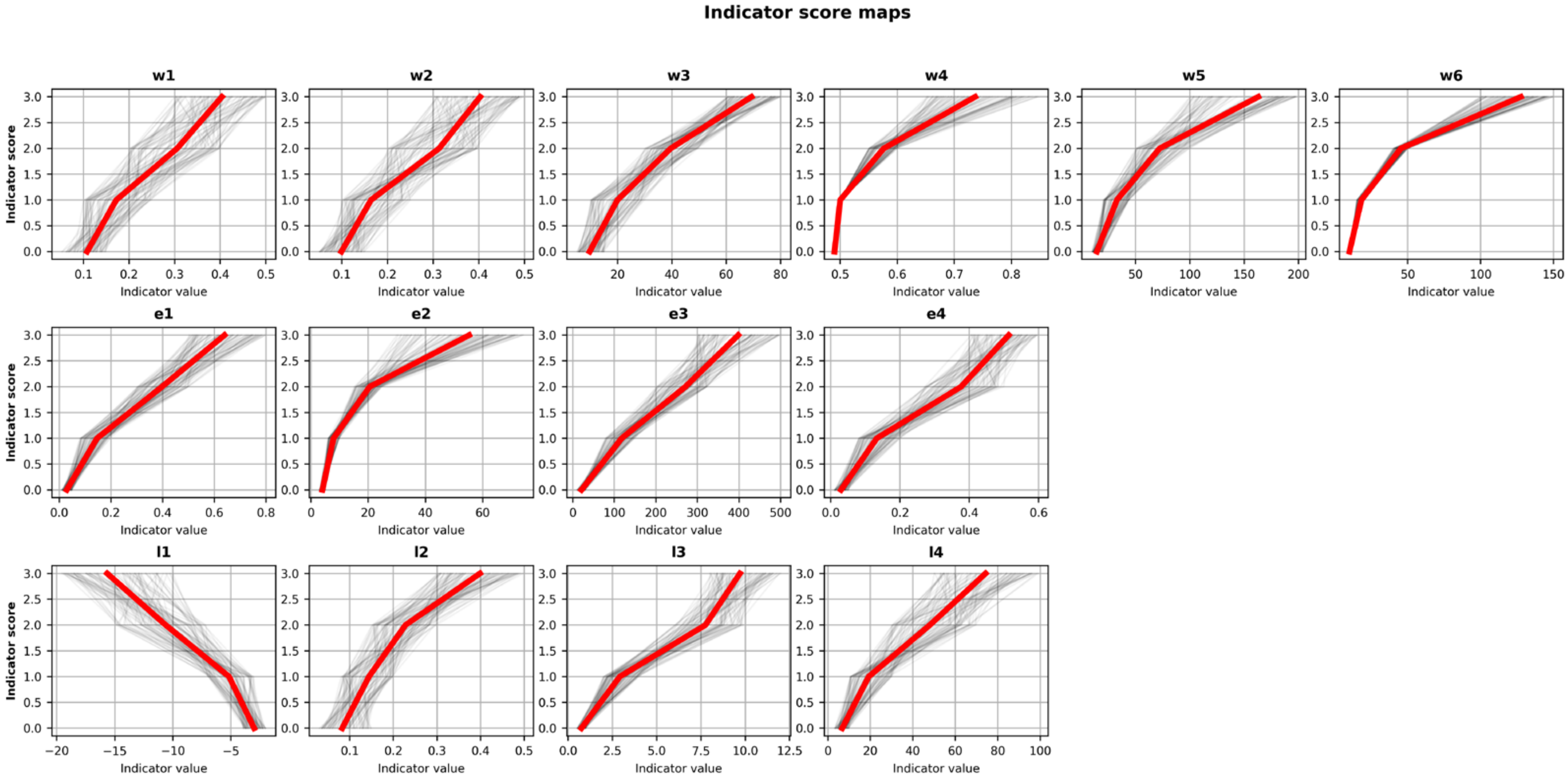

Figure S 5. Indicator score maps for each indicator. The grey lines show the 100 random sets of uniformly sampled values taken from the ranges in Table S 4.

1.7. Indicator scores

Water sector scores

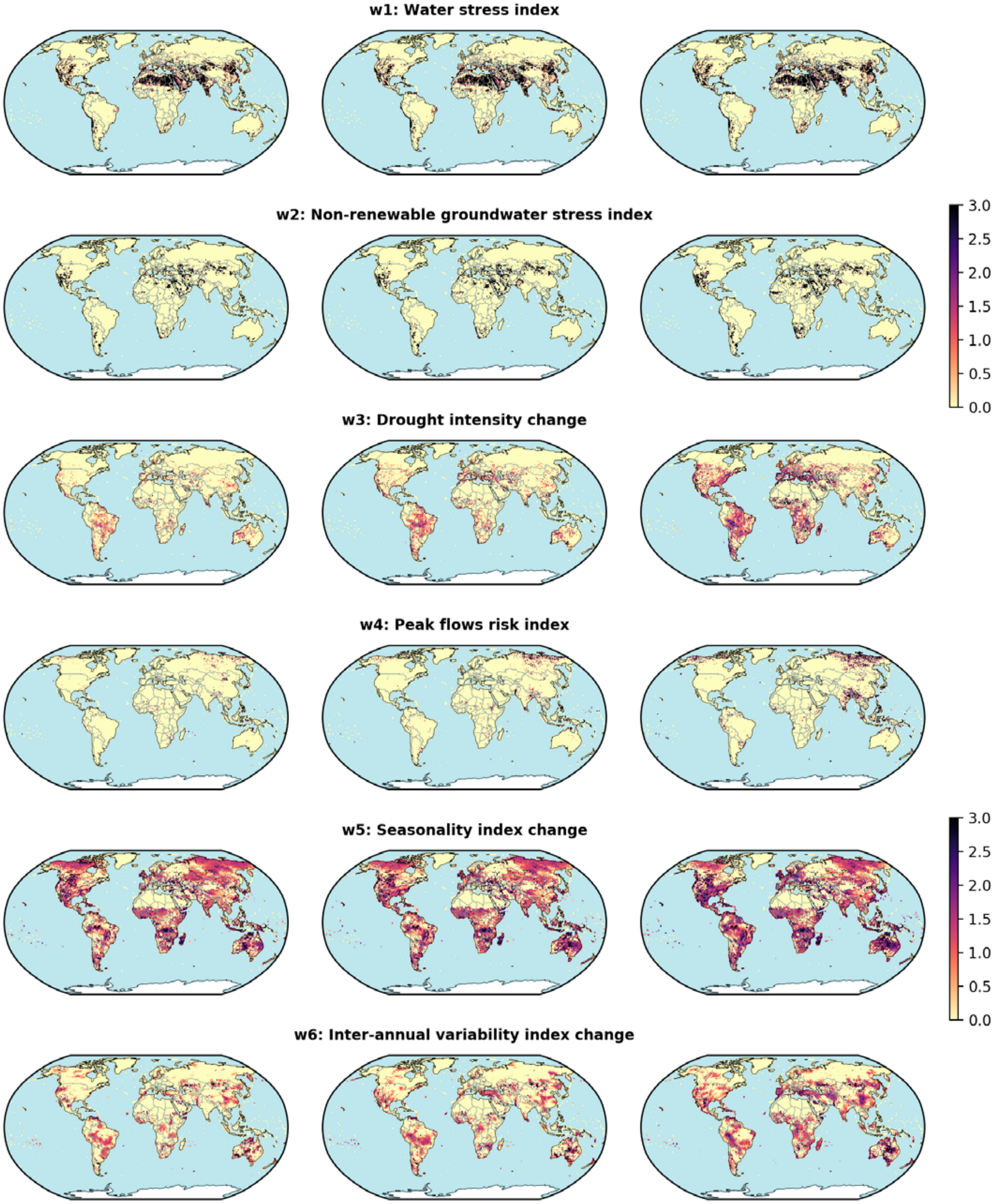

Figure S 6. Scores for the water sector indicators.

Energy sector scores

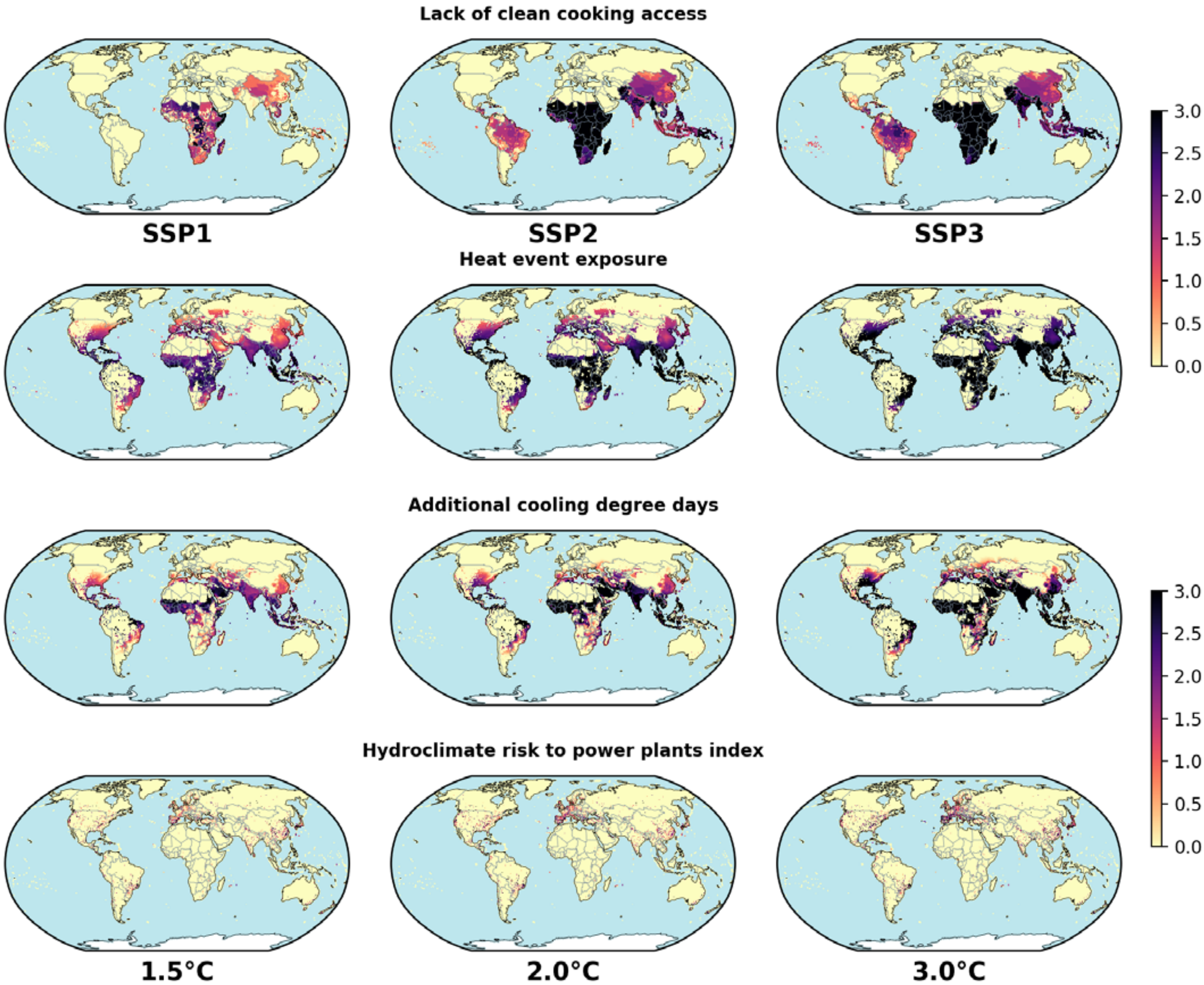

Figure S 7. Scores for the energy sector indicators.

Land sector

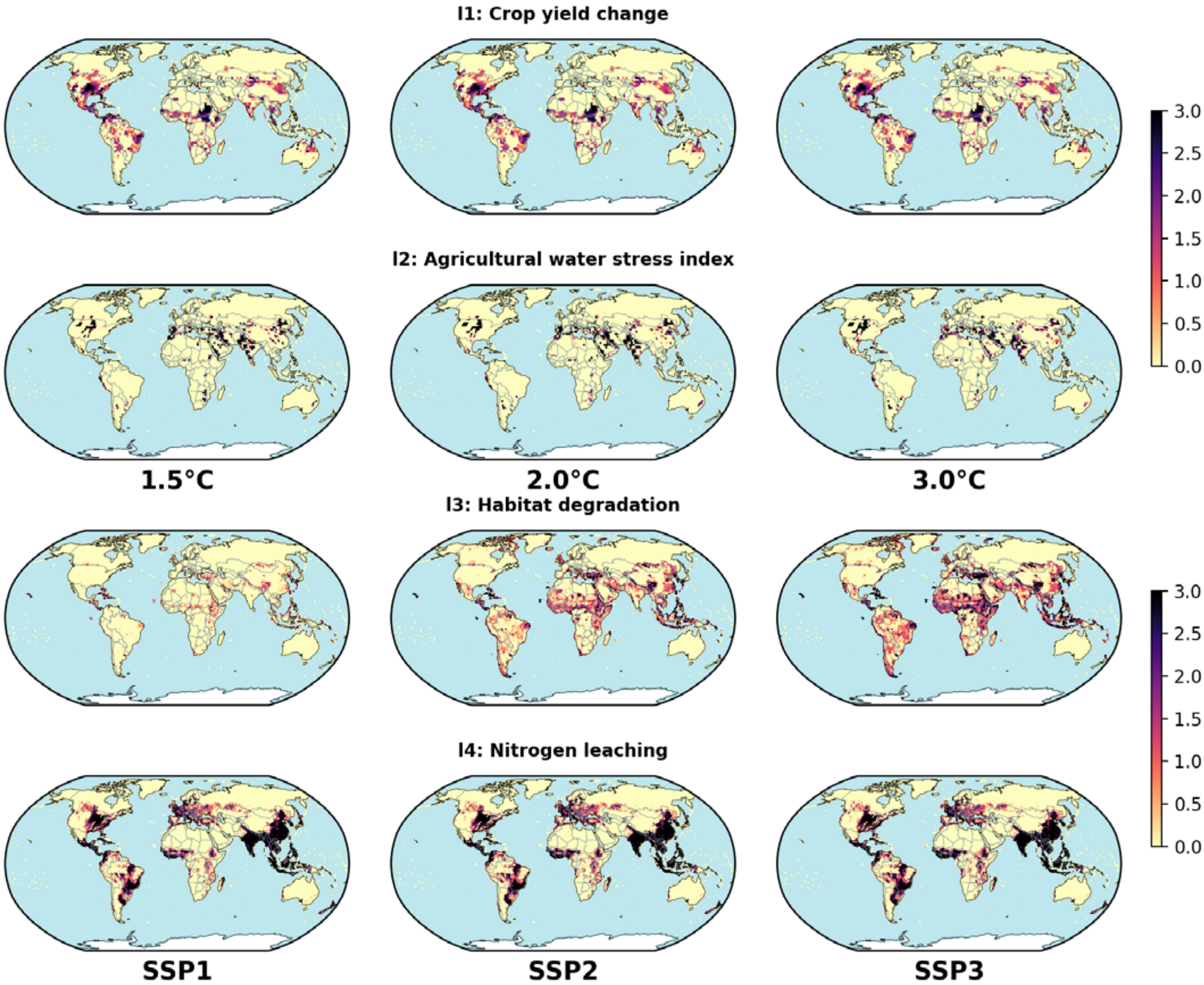

Figure S 8. Scores for the land sector indicators.

1.8. Sectoral score maps

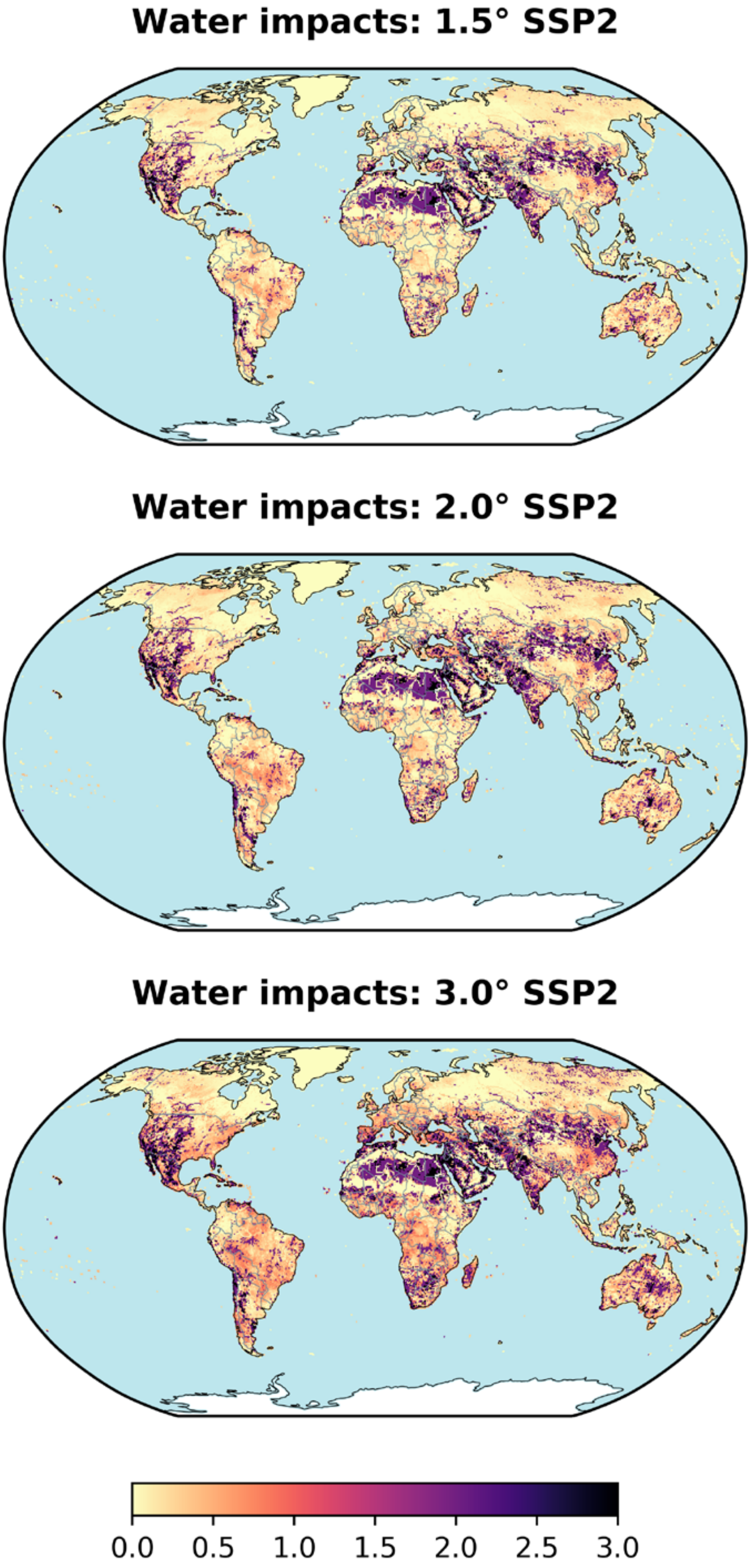

Figure S 9. Sectoral score maps for water.

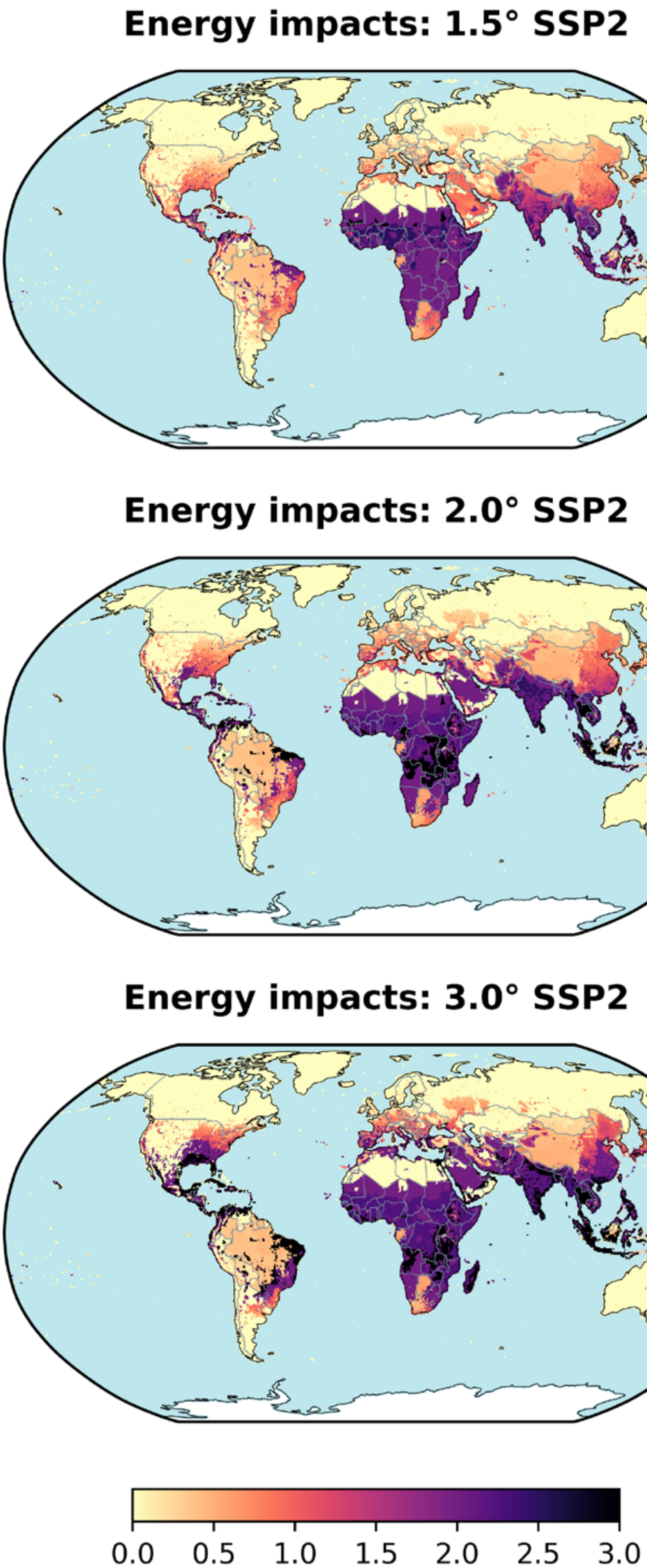

Figure S 10. Sectoral score maps for energy

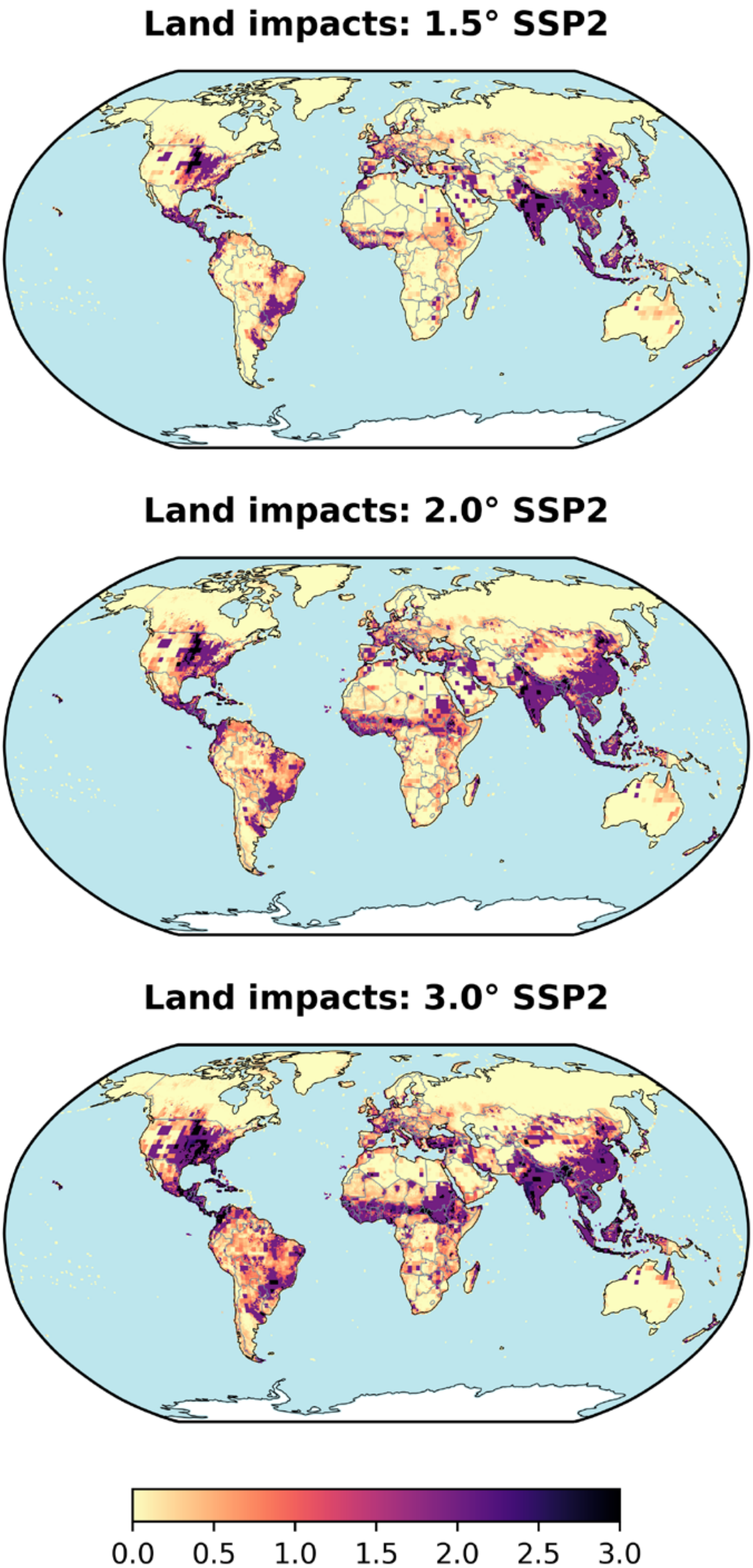

Figure S 11. Sectoral score maps for land

2. Multisector information

2.1. Multi-sector hotspot maps

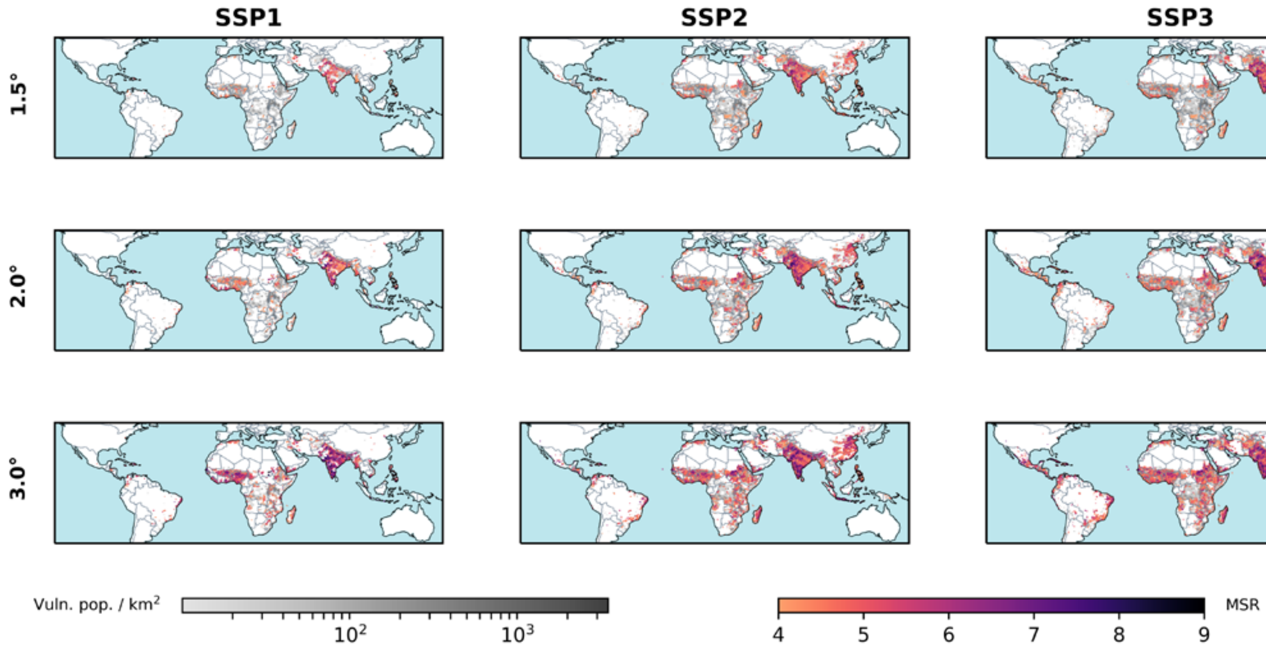

Figure S 12. Multi-sector hotspot maps for MSR≥4.0

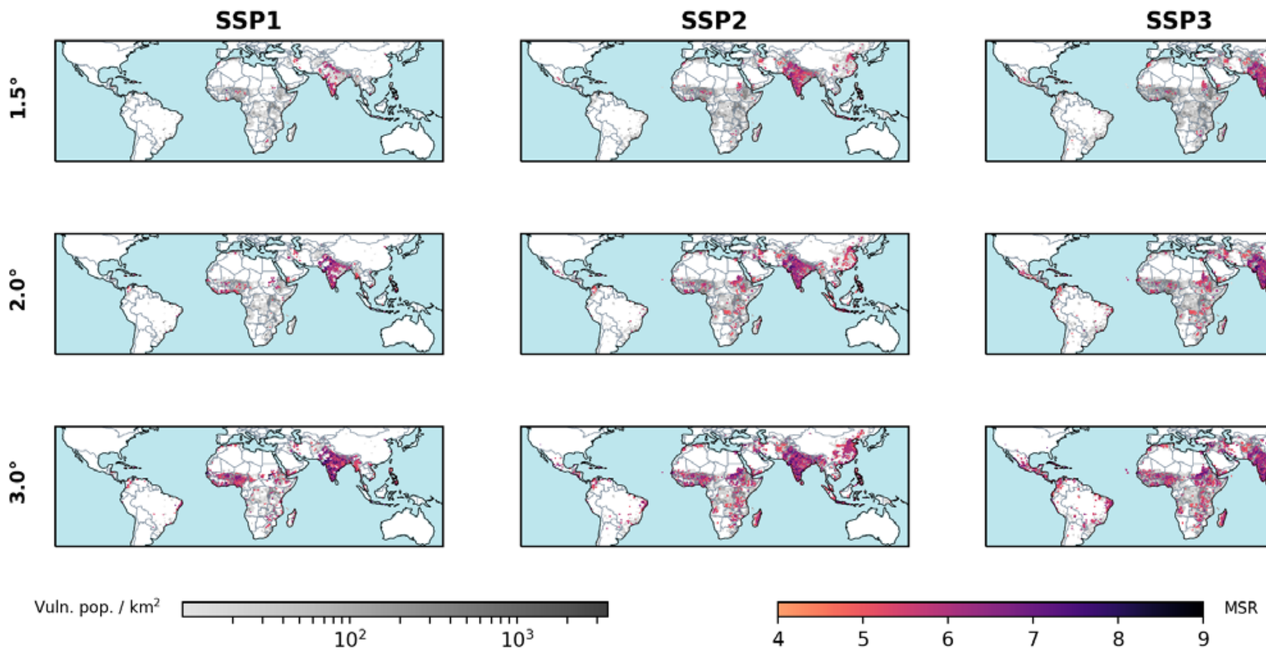

Figure S 13. Multi-sector hotspot maps for MSR≥5.0 (as in the manuscript).

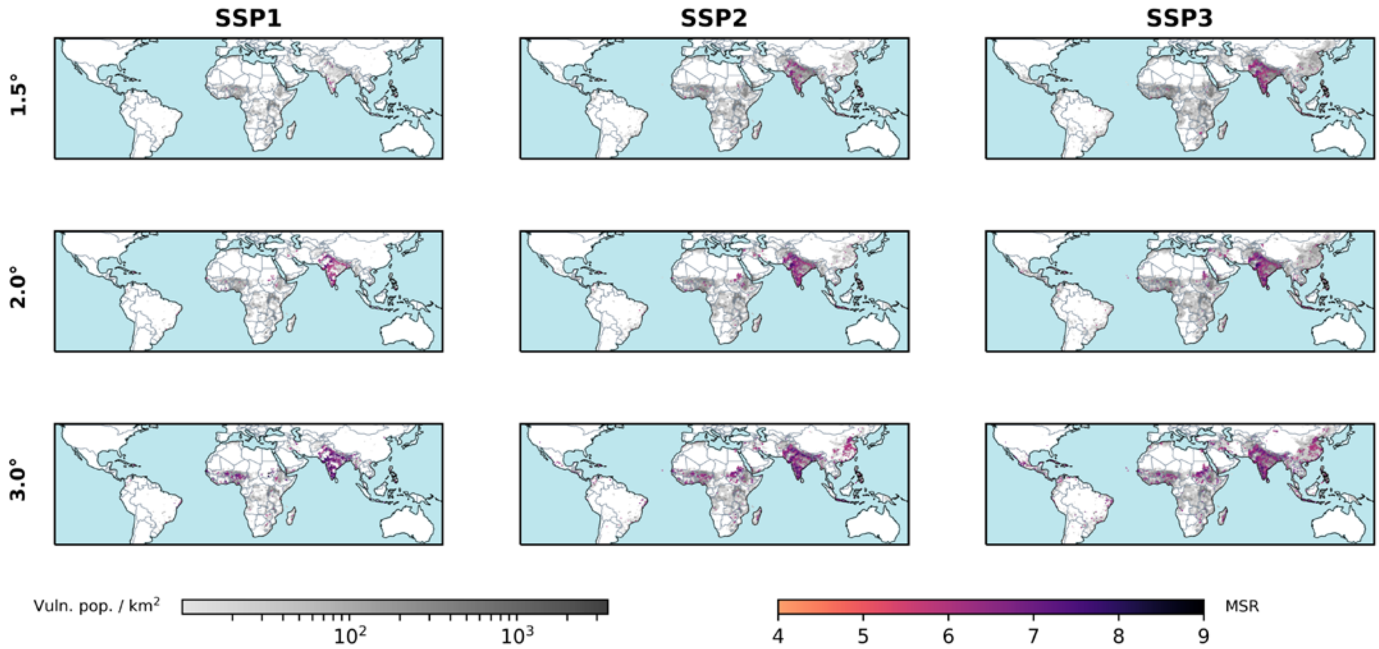

Figure S 14. Multi-sector hotspot maps for MSR≥6.0

3. Global exposure and vulnerability

3.1. Global population and vulnerable population

Additional methodological information

In this study, gridded projections of population and GDP for SSP 1-3 spanning 2010 to 2050 [48] at 0.125° resolution are used to identify the distribution and numbers of exposed and vulnerable populations. We use recently compiled datasets of global income distributions and inequality [17] to estimate vulnerable populations below various income thresholds. These datasets are generated for each SSP from 2010-2050 by first estimating future urban and rural income and inequality using machine-learning regression techniques, such as boosted regression trees. Given future pathways of national urban and rural income, inequality, and population, subnational estimates are generated using non-linear programming techniques that guarantee shares of very-low-income populations are consistent between national estimates and those projected for subnational units. Base year patterns of subnational income and inequality are generated from available data sources that cover 70% of today's population and are used to initiate the projection process for each country. Final estimates of state-level income and inequality for urban and rural populations are then combined with urbanization and migration patterns from the gridded population projections to produce gridded estimates of vulnerable populations (SI Figure S15).

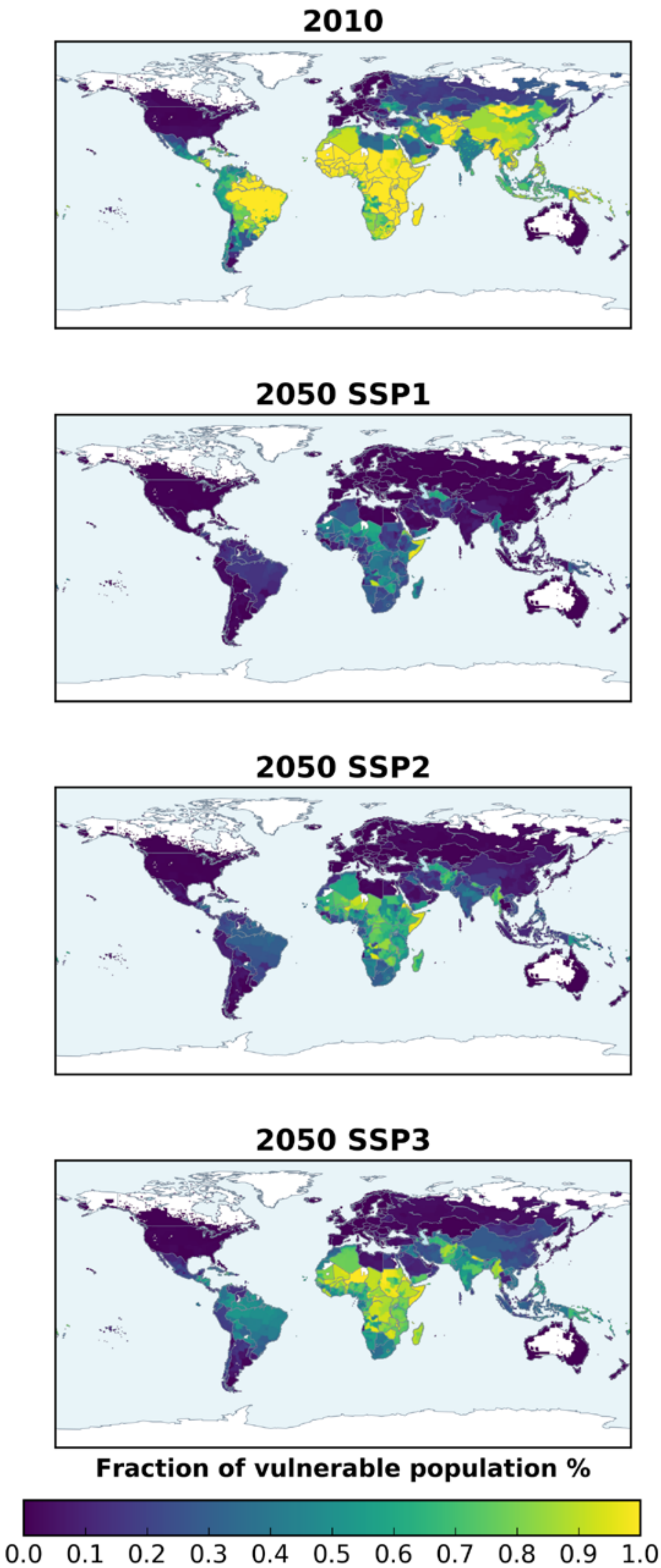

Figure S 15. Maps of the vulnerable population (income <$10 / day) for each SSP in 2010 and 2050.

3.2. Total, exposed and vulnerable population plots

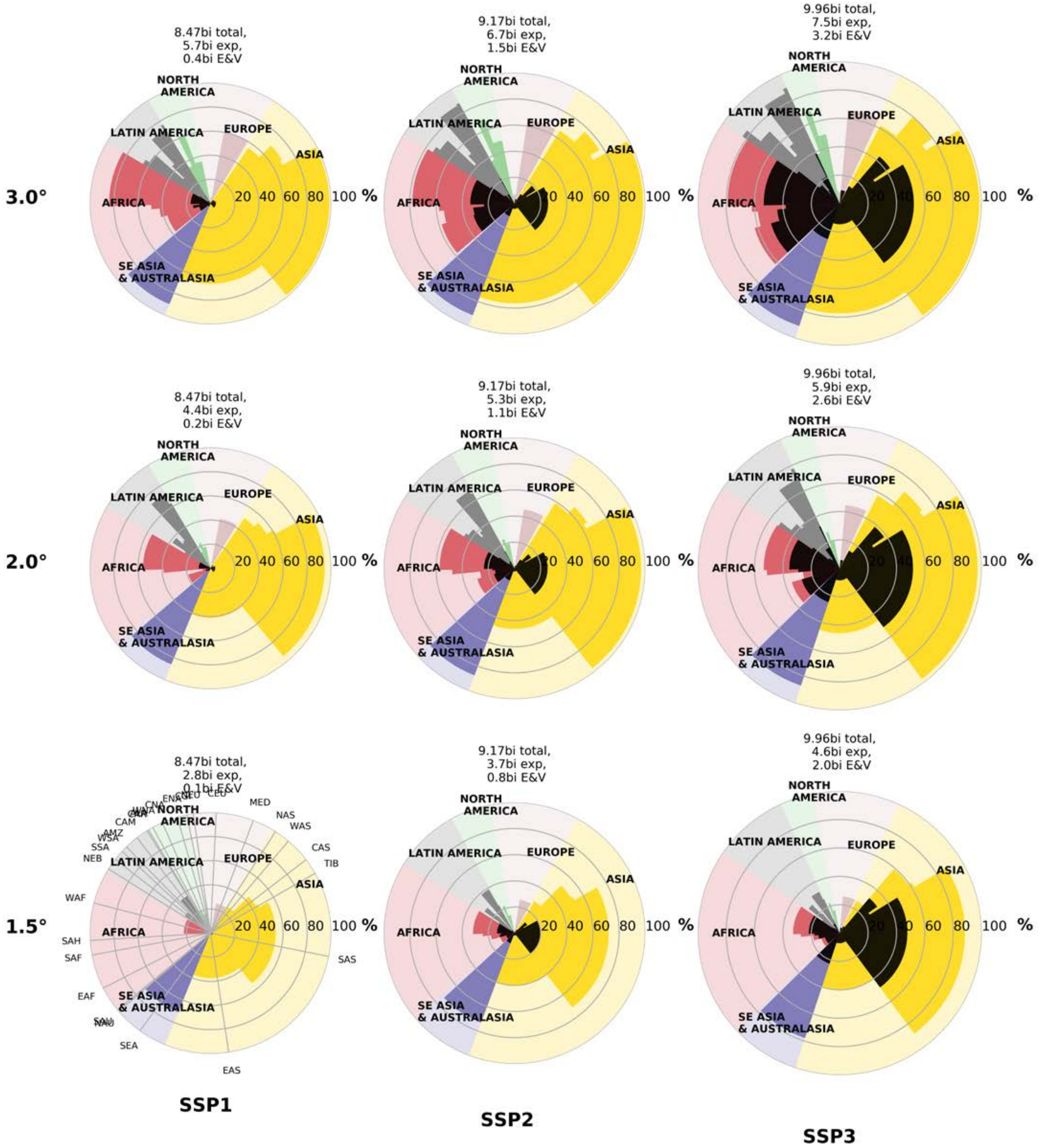

Figure S 16. Total, exposed and vulnerable population in 2050 for MSR≥4.0.

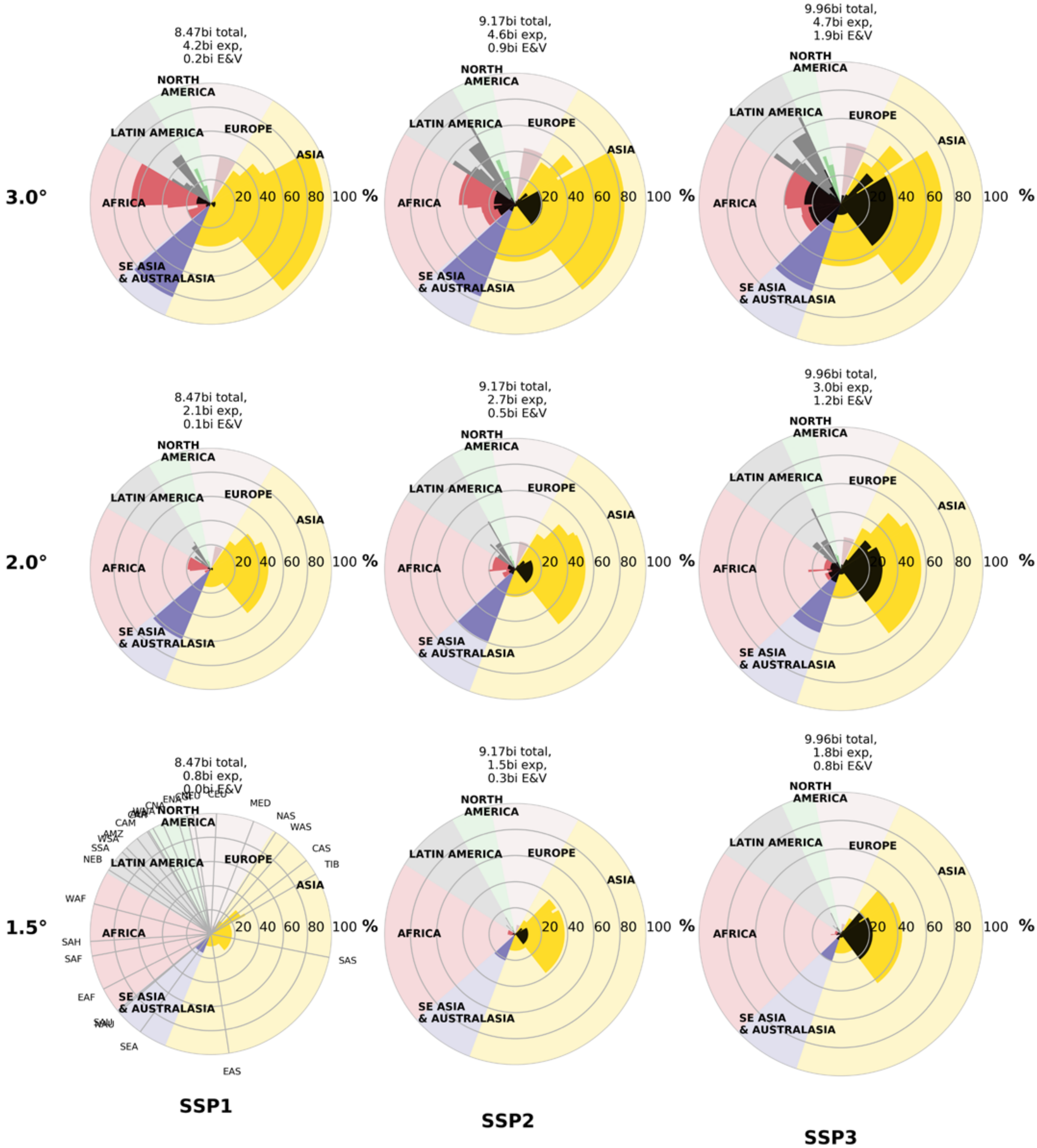

Figure S 17. Total, exposed and vulnerable population in 2050 for MSR≥5.0.

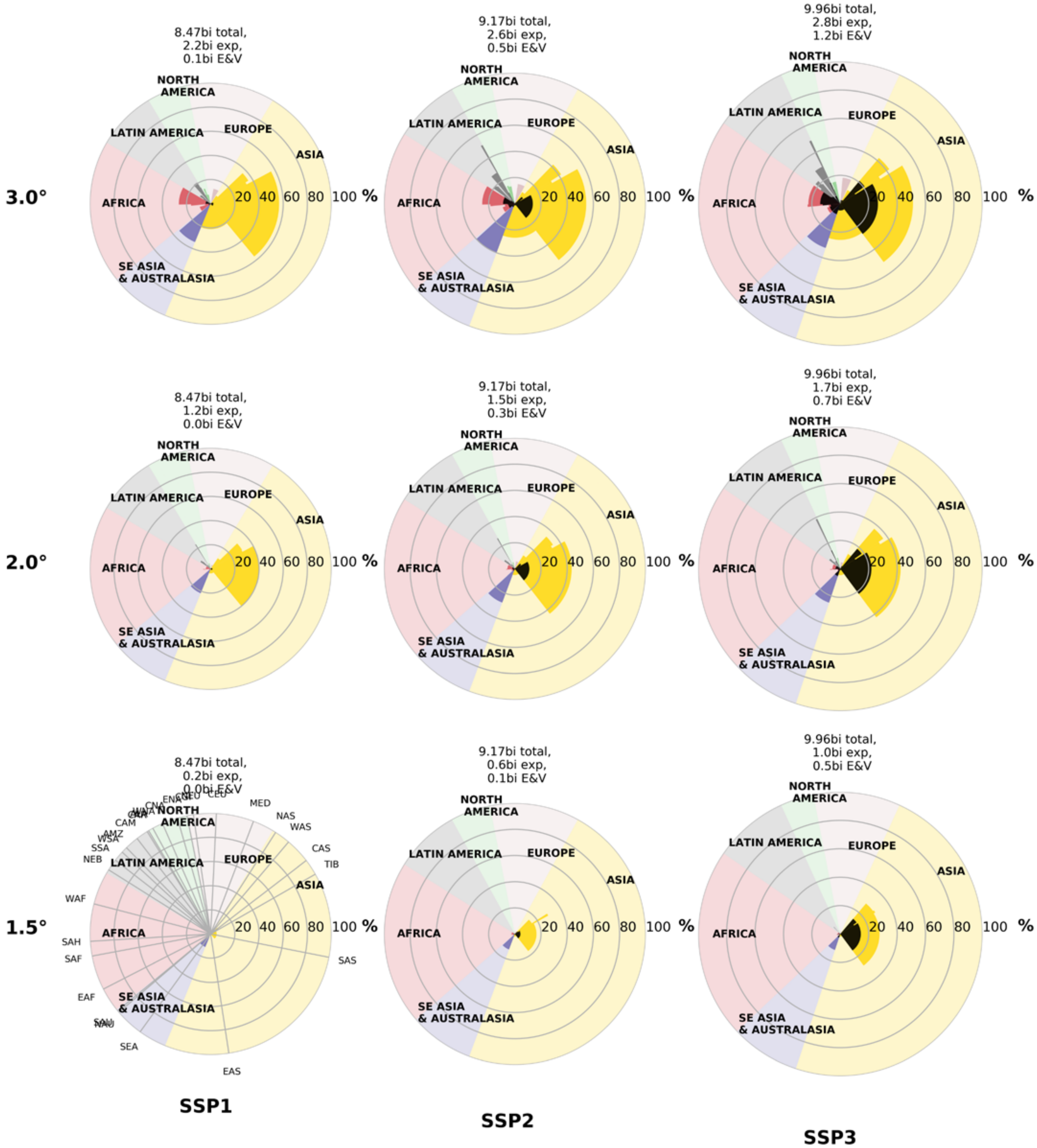

Figure S 18. Total, exposed and vulnerable population in 2050 for MSR≥6.0.

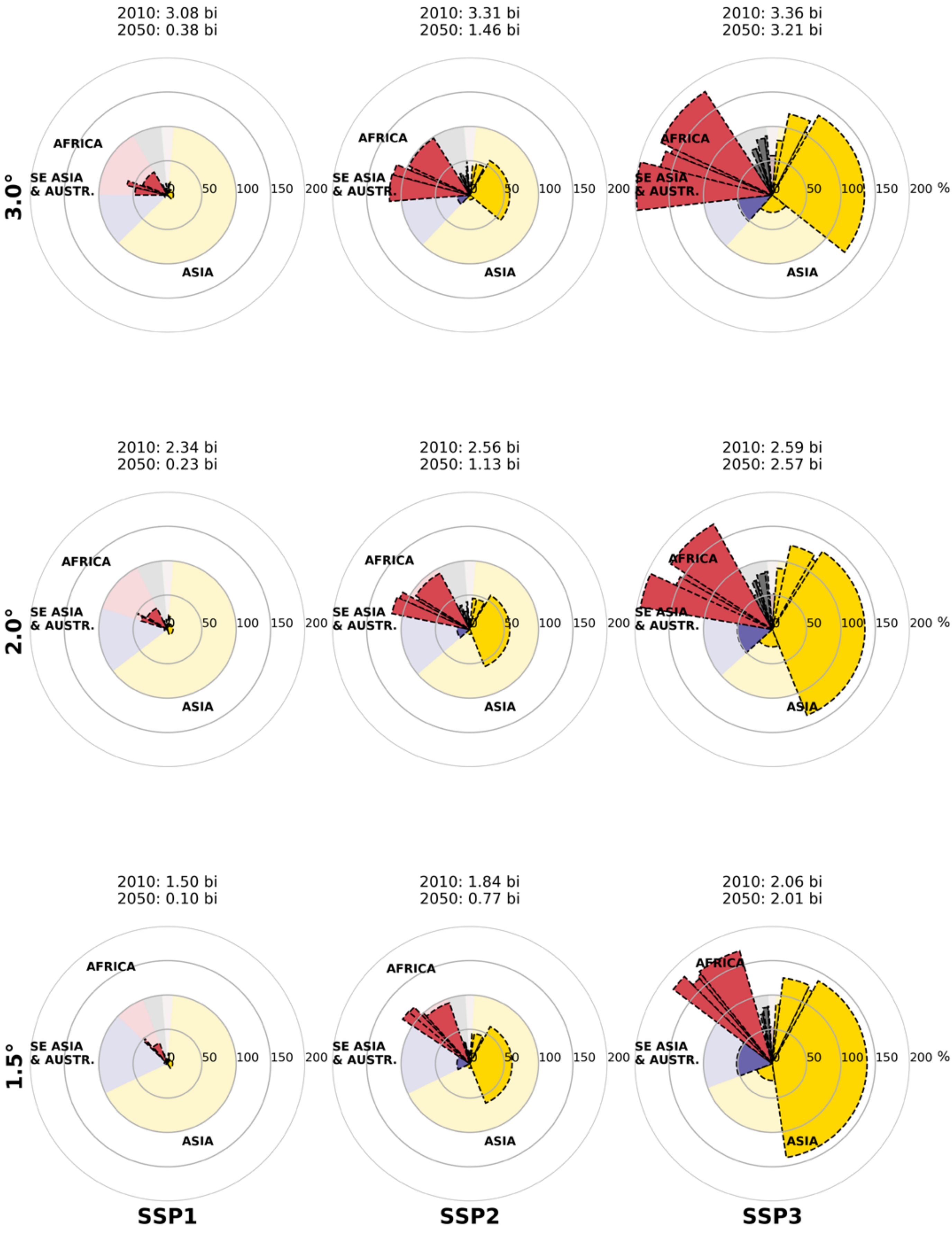

Figure S 19. Exposed and vulnerable population for MSR≥4.0 in 2010 and 2050.

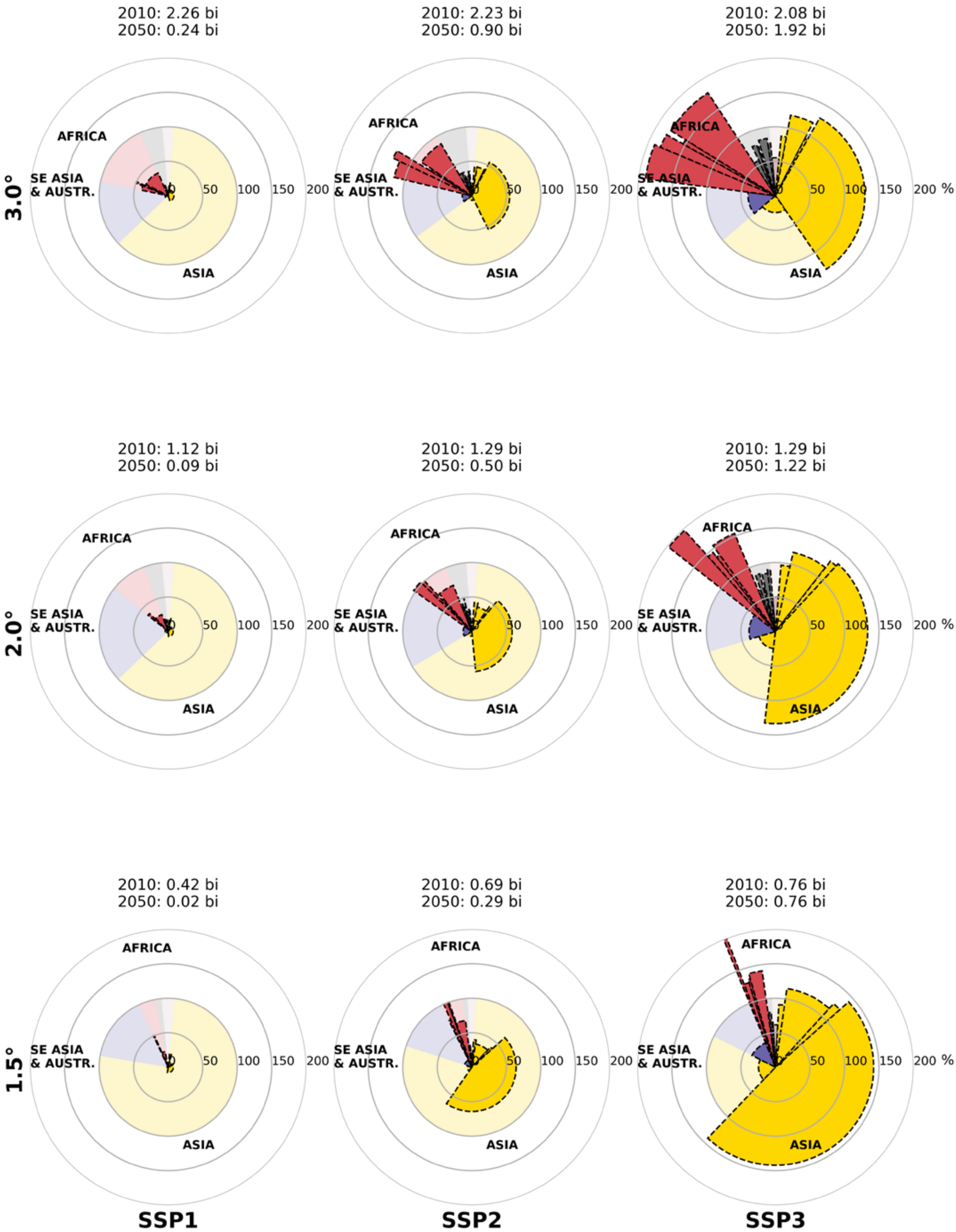

Figure S 20. Exposed and vulnerable population for MSR≥5.0 in 2010 and 2050.

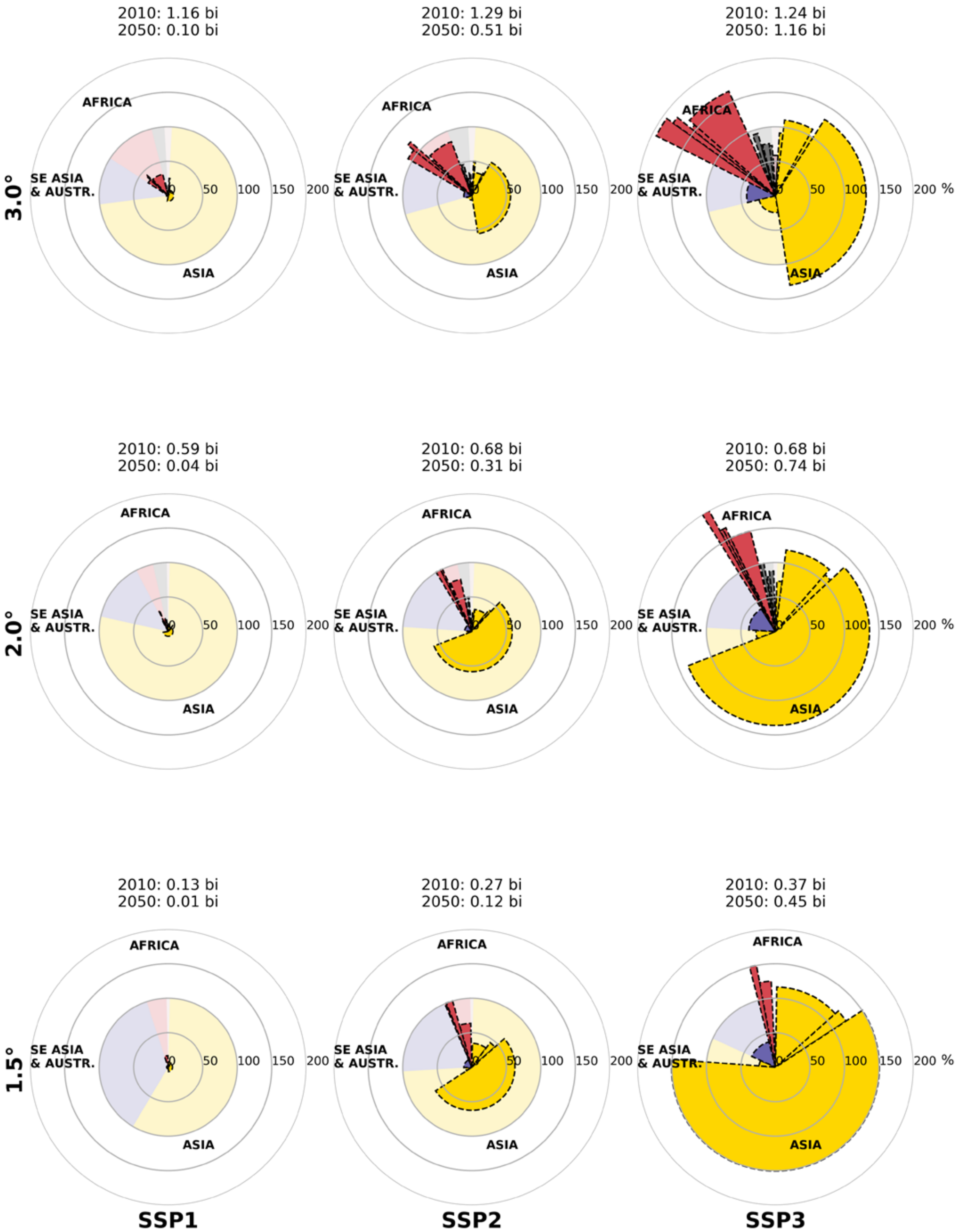

Figure S 21. Exposed and vulnerable population for MSR≥6.0 in 2010 and 2050.

3.3. Regional impacts distribution by populations

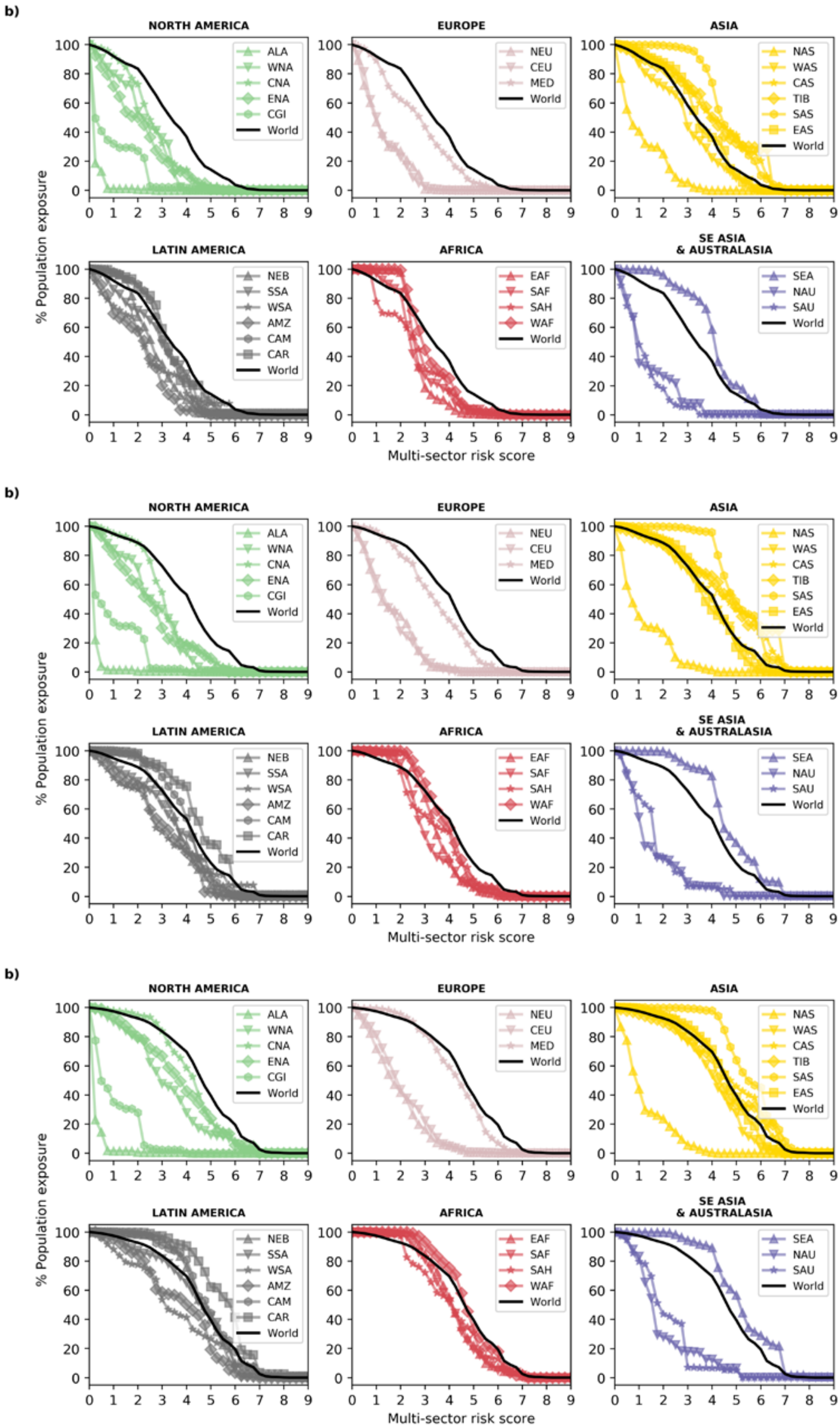

Figure S 22. Regional cumulative distribution functions for 1.5°, 2.0° and 3.0°C (top to bottom) for SSP2 population in 2050. Black line shows the global median and coloured lines show the regional distributions for the 27 IPCC SREX regions for 1.5, 2.0 and 3.0°C (top to bottom). As the climate warms, the impact distributions move further to the right. The distance between impacts benign and impacts severe regions also grows.

3.4. Analysis by latitude

An analysis by latitude was performed when investigating the land and population related impacts. Results were calculated at 0.5° resolution but are plotted as a 2° rolling average in Figure S 23 for smoothing.

i. Mean pixel score is calculated as the average MSR score of all land pixels at that latitude.
ii. Cumulative unweighted pixel score is the sum of MSR score for all land pixels at that latitude.
iii. Land area weighted is the same as (ii) but weighted to account for the changing areas of pixels at latitudes further from the equator.
iv. For Population weighted first the global population in each pixel was rescaled to between 1-0 using MinMax rescaling (ref) and then multiplies by the pixel MSR scores.

The MSR threshold line is equivalent to every land pixel in that latitude have a score at the threshold (MSR=5.0). It is intended to give a common reference point between the figures.

Across the 4 panels (Figure S 23), the space between 40°N and the equator consistently face the worst risks, whether on an (i) average, (ii) unweighted cumulative, (iii) land area-weighted cumulative, (iv) or population-weighted cumulative basis. Outside of 40°N/S scores drop off substantially. Excluding the tropics, northern hemisphere scores are considerably less than southern hemisphere impacts, indicated by the larger distances (to the left) from the MSR threshold line. The latitudes 15°N to 5°N are consistently closest to the MSR line indicating that at these latitudes all pixels are expected to experience, on average, multi-sector risks.

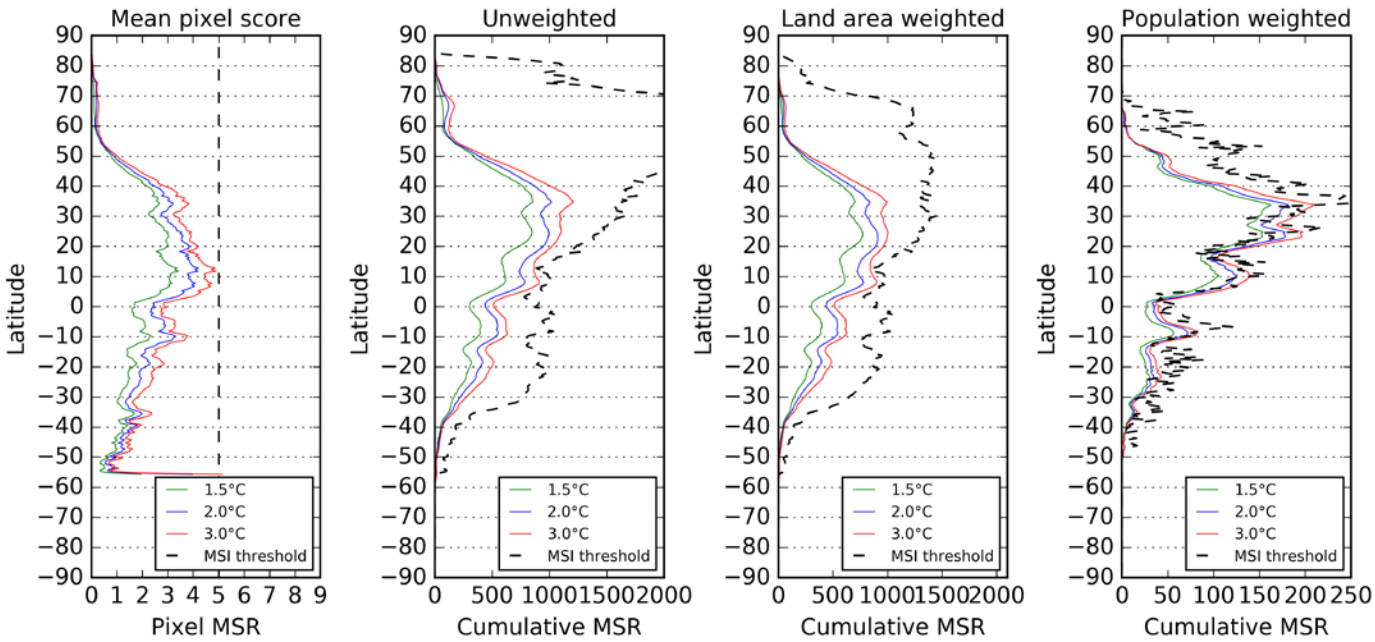

Figure S 23. Multi-sector impact scores by latitude show the difference that latitude makes for exposure of negative climate impacts.

3.5. Sensitivity of population exposure to MSR level

Sensitivity of exposure for the global and the exposed and vulnerable (E&V) populations was tested by varying the MSR between 4-6, making comparison to the 1.5°C equivalent scenario. The y-axis indicates the multiplier factor for exposed population compared to the 1.5°C case.

For the exposed population, there is little difference between SSPs because the main change between the scenarios is the total population count. However, the fact that the dotted lines for E&V are above the global exposed lines (solid lines), shows that the E&V population grows more (proportionally) than the exposed population. The difference between the dotted lines are the SSPs. In each GMT the upper dotted lines are for SSP3, indicating that in this SSP, the E&V population is substantially more exposed compared to the global exposure.

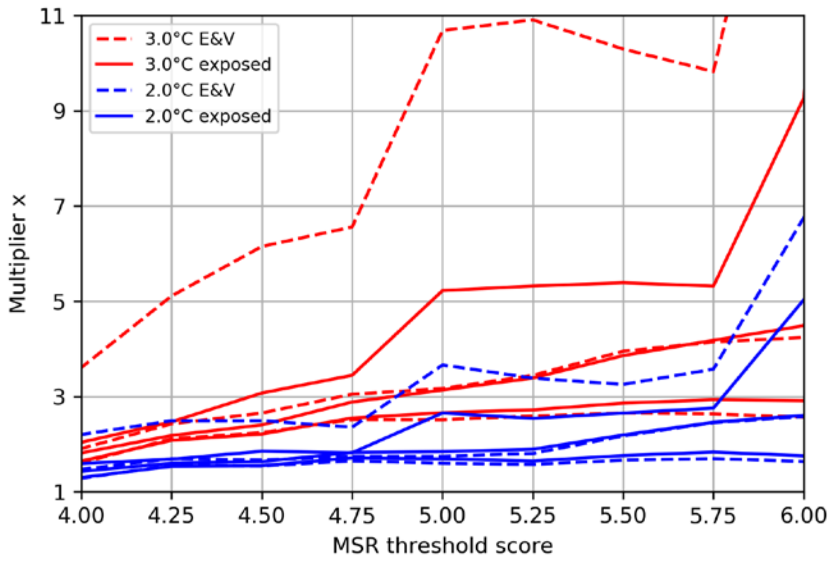

Figure S 24. Sensitivity of exposure for the global and the exposed and vulnerable (E&V), at 2.0 and 3.0°C warming compared to 1.5°C – with 3 SSPs in each case.

4. Uncertainty and pairwise correlation analyses

4.1. Component uncertainty analysis

We undertook an uncertainty analysis following the approach of Hawkins & Sutton (2009)[1] , to determine the variability (through coefficient of variation) across the key components of GCM, Impact Model, Score Range, GMT and SSP. This was systematically assessed for every indicator, the combined sectoral scores of water, energy and land, and the combined hotspot score.

The process identifies for each indicator the magnitude of component uncertainty that derives from the different model variants and scenario combinations (hereafter variants). For each uncertainty component, the coefficient of variation (RSD) across variants was calculated, keeping all other uncertainty components constant in the central scenario (ensemble mean of GCMs, ensemble mean of impact models, 50th percentile across the score range combinations, 2.0°C global mean temperature, and SSP2 pathway)(Table S 5).

In each variant, the number of gridsquares with a score above the moderate risk threshold was counted (in all cases $s_i \geq 2$ apart from the hotspot score $M\ s_i \geq 4$).

For the GCMs and Impact models, the assessment is useful for establishing the sources of model uncertainty (including individual GCMs and Impact Models) compared to the ensemble mean, including where efforts to improve models can be focused. For the Score Ranges, the assessment quantifies and compares the extent of expert uncertainty, one of the more subjective aspects of this study. For the GMTs and SSPs, the assessment indicates the sensitivity to this scenario uncertainty.

Table S 5. Central case and variants used in the uncertainty analysis.

	Uncertainty components				
	GCMs	**Impact Models**	**Score Range**	**Global Mean Temperature**	**SSPs**
Central case	Ensemble mean	Ensemble mean	*50th percentile ($p_{50,}$)*	2.0°C	SSP2
Variants	Individual GCMs*	Individual impact models*	p_5, p_{25}, p_{50}, p_{75}, p_{95}	1.5°C, 2.0°C, 3.0°C,	SSP1, SSP2, SSP3
# variants	63	32	*90*	51	54

* Variants where applicable and available

The assessment was carried out at three exposure subsets:

- All land gridsquares (~65,000) (Figure S 25).
- Gridsquares with population density > 10 people/km^2 (~20-23,000 potential gridsquares, depending on SSP) (Figure S 26).
- Gridsquares with vulnerable population density > 10 people/km^2 (~5-12,000 potential gridsquares, depending on SSP) (Figure S 27)

In each case, before summation the count of gridsquares was weighted by gridsquare area, to take into account the changing gridsquare area by latitude. For example, a gridsquare at the equator is weighted by 1, whilst a gridsquare on the Tropic of Cancer/Capricorn (23.5° N/S latitude) is weighted by 0.92, and a location at 45° N/S latitude is weighted by 0.71. Not performing this area weighting over-emphasises uncertainties at high latitudes where gridsquare areas are small and population density low.

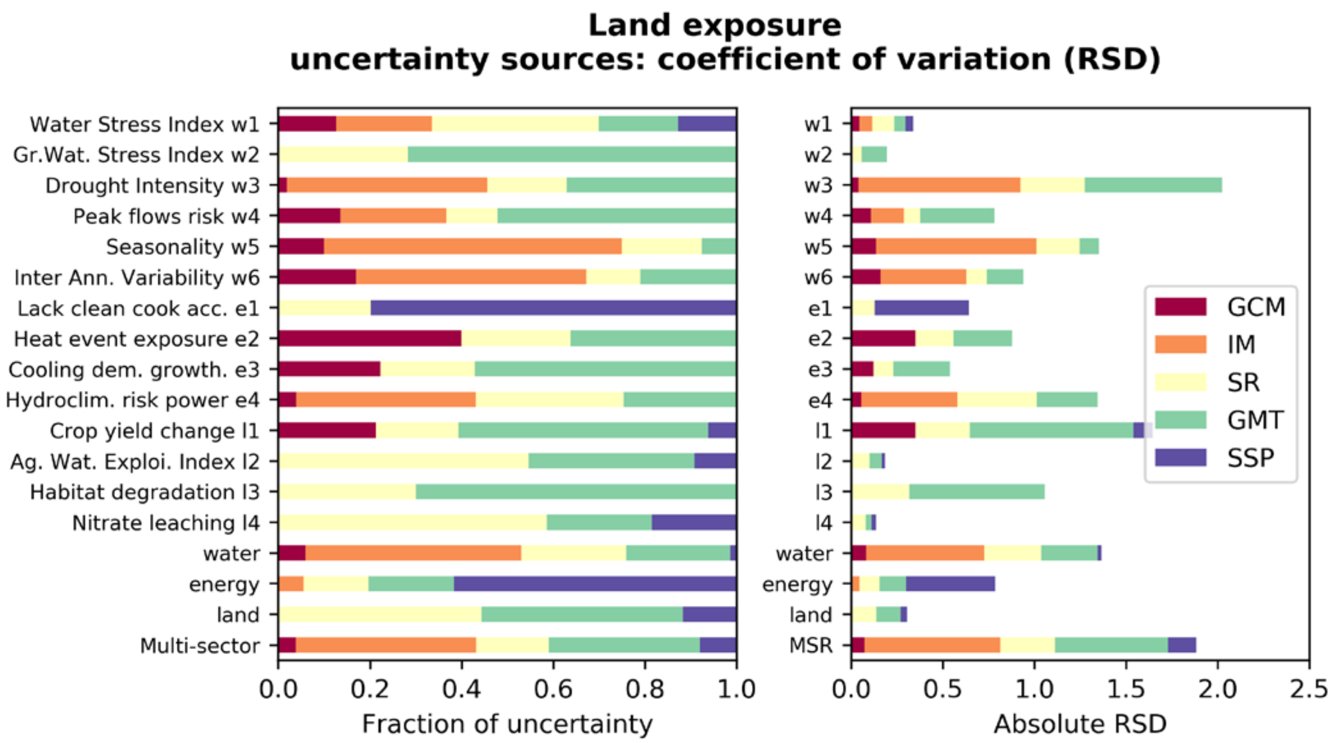

Figure S 25. Uncertainty sources in the sensitivity of number of gridsquares moderately impacted, for all Land gridsquares.

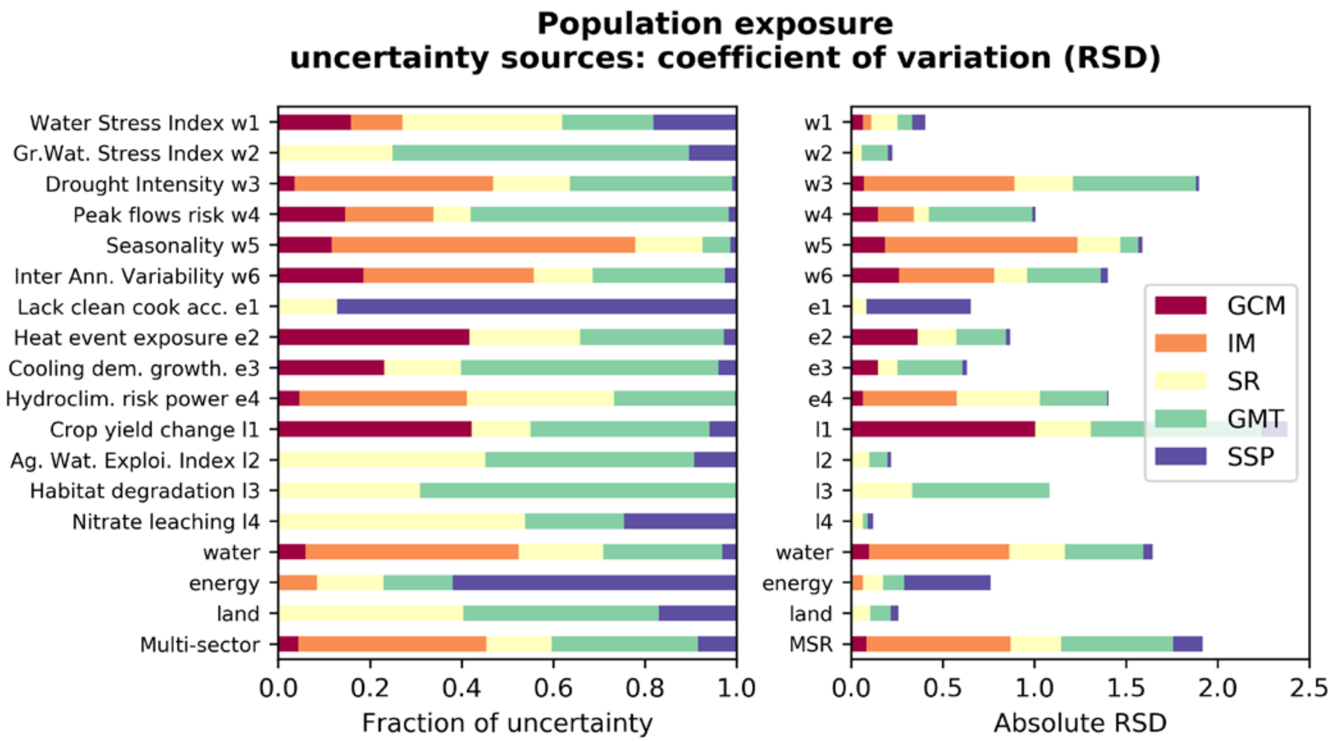

Figure S 26. Uncertainty sources in the sensitivity of number of gridsquares moderately impacted, for gridsquares with population density ≥ 10 people / km^2.

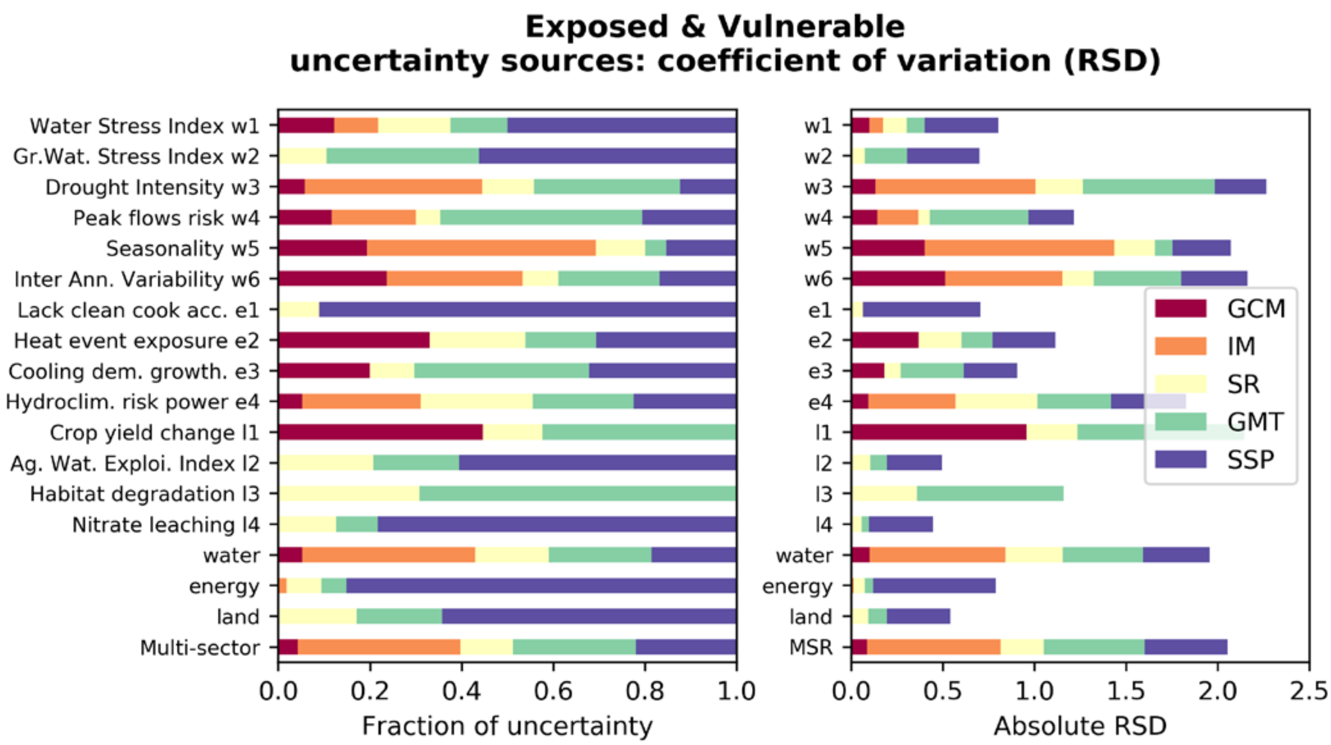

Figure S 27. Uncertainty sources in the sensitivity of number of gridsquares moderately impacted, for all gridsquares with vulnerable population density ≥ 10 people / km^2.

4.2. Pairwise correlation analysis

A pairwise correlation analysis was undertaken to better understand the correlation structure between the indicator scores. This analysis serves two purposes:

i. to determine whether any pairs of related indicators are so highly correlated that in effect one of them is redundant. For example, heat events and cooling demand growth, both derive from temperature data and could (mistakenly) be considered as double-counting. Extremely high correlations, e.g. above 0.95 would confirm this. However, the former is based on the right tail whilst cooling demand growth uses a much larger portion of the distribution.
ii. to identify pairs of less obviously related indicators that correlate to indicate lines of further analysis. For example,

Similar to the uncertainty analysis, the pairwise correlation analysis is presented for the central scenario of 2.0°C and SSP2 in 2010 and 2050, across three exposure perspectives (Figure S 28:

- All land gridsquares (~65,000).
- Gridsquares with population density ≥ 10 people/km^2 (~20-23,000 potential gridsquares, depending on SSP).
- Gridsquares with vulnerable population density ≥ 10 people/km^2 (~5-12,000 potential gridsquares, depending on SSP).

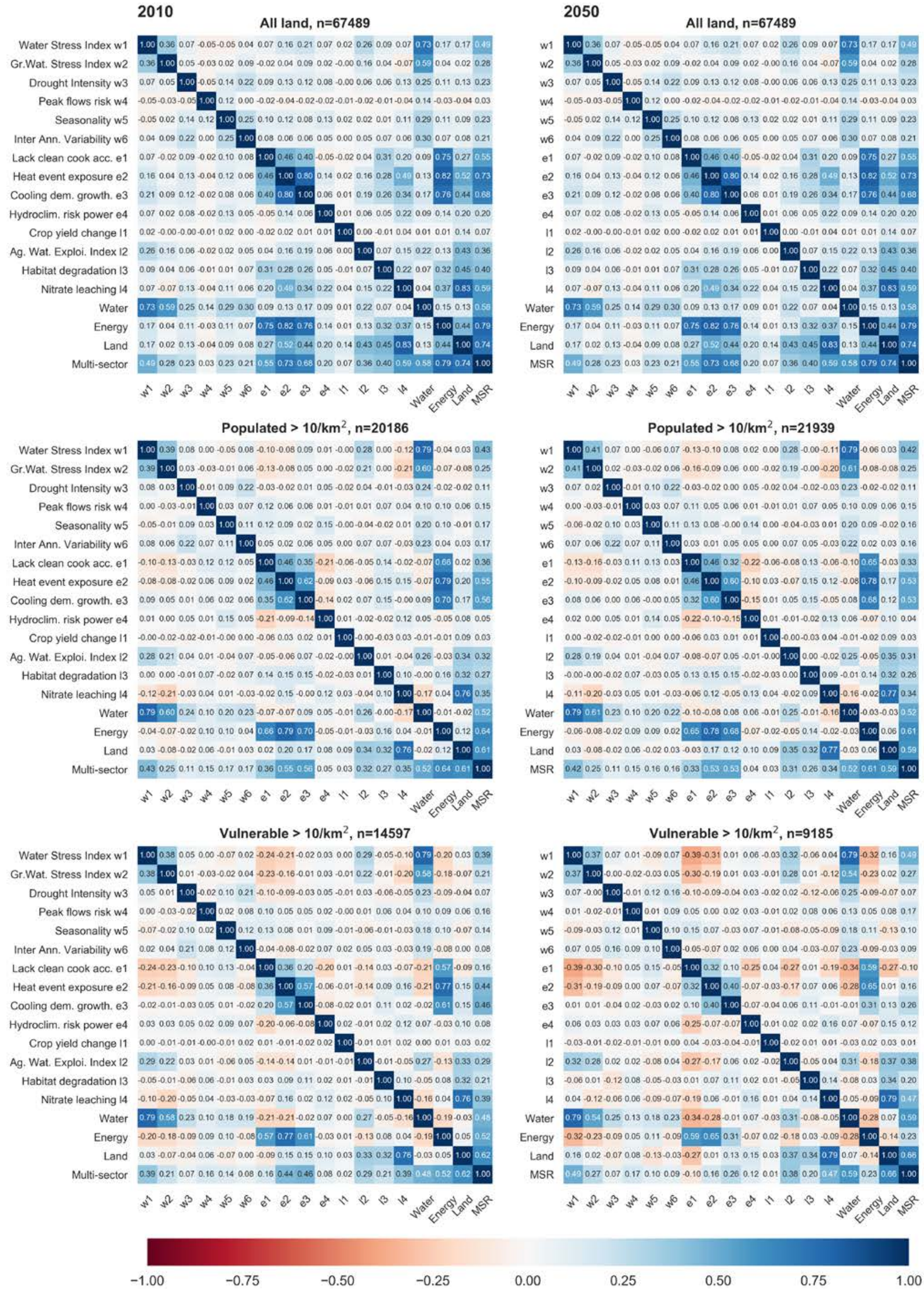

Figure S 28. Pairwise correlation heatmaps for SSP2 and 2.0°C for both 2010 and 2050 populations.

5. Tables of population exposure and vulnerability

Table S 6. Multi-sectoral exposed population by IPCC region for MSR≥5.0 in 2050. (millions of people)

LAB	NAME	IPPC #	REGION	SSP 1				SSP2				SSP3			
				1.5°C	2.0°C	3.0°C	2-1.5°C	1.5°C	2.0°C	3.0°C	2-1.5°C	1.5°C	2.0°C	3.0°C	2-1.5°C
ALA	Alaska/N.W. Canada	1	1	0	0	0	0	0	0	0	0	0	0	0	0
WNA	West North America	3	1	1	1	16	1	0	1	17	1	0	2	15	2
CNA	Central North America	4	1	4	11	42	7	8	14	47	6	4	12	38	8
ENA	East North America	5	1	1	14	34	12	1	14	55	12	3	17	50	15
CGI	Canada/Greenl./Iceland	2	1	0	0	0	0	0	0	0	0	0	0	0	0
NEU	North Europe	11	2	0	0	0	0	0	0	0	0	0	0	0	0
CEU	Central Europe	12	2	0	0	3	0	0	0	8	0	0	0	7	0
MED	South Europe/ Mediterr.	13	2	33	91	188	58	36	108	219	72	39	121	232	82
NAS	North Asia	18	3	0	0	0	0	0	0	0	0	0	0	0	0
WAS	West Asia	19	3	37	79	94	41	39	99	117	61	44	113	116	70
CAS	Central Asia	20	3	83	122	139	38	126	162	178	36	165	209	217	44
TIB	Tibetan Plateau	21	3	25	32	39	7	28	45	32	17	39	55	36	16
SAS	South Asia	23	3	322	878	1723	557	780	1108	1721	327	1014	1329	1673	315
EAS	East Asia	22	3	148	219	514	71	190	318	659	128	207	318	669	111
SEA	Southeast Asia	24	4	107	401	533	294	148	408	520	260	149	355	485	207
NAU	North Australia	25	4	0	0	1	0	0	0	1	0	0	0	1	0
SAU	South Australia/ New Z.	26	4	0	0	2	0	0	0	2	0	0	0	1	0
EAF	East Africa	16	5	5	29	111	24	9	65	162	56	9	88	217	79
SAF	Southern Africa	17	5	1	0	26	-1	11	18	68	8	10	26	82	16
SAH	Sahara	14	5	2	17	35	14	6	22	39	16	8	26	43	19
WAF	West Africa	15	5	25	143	492	118	49	149	368	100	42	118	395	76
NEB	North-East Brazil	8	6	0	8	32	8	0	15	52	15	0	15	58	15
SSA	SE South America	10	6	0	29	47	29	1	31	79	30	1	54	94	53
WSA	W. Coast South America	9	6	5	6	13	1	6	17	24	11	6	19	29	13
AMZ	Amazon	7	6	0	2	15	2	1	4	21	3	1	5	27	4
CAM	Central America/Mexico	6	6	5	55	111	50	9	61	143	52	17	72	173	55
CAR	Small Islands Reg. Caribb.	27	6	3	10	18	8	6	17	29	11	8	23	33	15
Total				**807**	**2147**	**4228**	**1339**	**1454**	**2676**	**4561**	**1222**	**1766**	**2977**	**4691**	**1215**

Table S 7. Multi-sectoral exposed & vulnerable population by IPCC region for MSR≥5.0 in 2050 and income ≤ $10/day. (millions of people)

LAB	NAME	IPPC #	REGION	SSP 1				SSP2				SSP3			
				1.5°C	2.0°C	3.0°C	2-1.5°C	1.5°C	2.0°C	3.0°C	2-1.5°C	1.5°C	2.0°C	3.0°C	2-1.5°C
ALA	Alaska/N.W. Canada	1	1	0	0	0	0	0	0	0	0	0	0	0	0
WNA	West North America	3	1	0	0	0	0	0	0	0	0	0	0	0	0
CNA	Central North America	4	1	0	0	0	0	0	0	0	0	0	0	0	0
ENA	East North America	5	1	0	0	0	0	0	0	0	0	0	0	0	0
CGI	Canada/Greenl./Iceland	2	1	0	0	0	0	0	0	0	0	0	0	0	0
NEU	North Europe	11	2	0	0	0	0	0	0	0	0	0	0	0	0
CEU	Central Europe	12	2	0	0	0	0	0	0	0	0	0	0	0	0
MED	South Europe/ Mediterr.	13	2	1	2	4	0	3	5	11	2	8	17	33	9
NAS	North Asia	18	3	0	0	0	0	0	0	0	0	0	0	0	0
WAS	West Asia	19	3	2	4	5	3	4	11	14	8	10	27	26	17
CAS	Central Asia	20	3	3	4	6	1	22	30	39	8	83	107	114	24
TIB	Tibetan Plateau	21	3	1	1	1	0	4	7	5	2	15	22	13	7
SAS	South Asia	23	3	11	31	72	21	205	282	428	77	526	688	869	162
EAS	East Asia	22	3	1	1	3	0	9	16	33	7	38	59	120	22
SEA	Southeast Asia	24	4	1	11	15	9	10	30	43	20	33	76	110	42
NAU	North Australia	25	4	0	0	0	0	0	0	0	0	0	0	0	0
SAU	South Australia/ New Z.	26	4	0	0	0	0	0	0	0	0	0	0	0	0
EAF	East Africa	16	5	1	6	24	5	3	33	88	30	6	69	171	63
SAF	Southern Africa	17	5	0	0	8	0	7	10	43	3	9	19	67	10
SAH	Sahara	14	5	0	1	4	1	2	5	11	3	4	11	23	7
WAF	West Africa	15	5	3	19	89	16	15	49	139	35	24	74	257	50
NEB	North-East Brazil	8	6	0	1	5	1	0	5	16	5	0	7	26	7
SSA	SE South America	10	6	0	2	3	2	0	4	10	4	0	13	22	13
WSA	W. Coast South America	9	6	0	0	0	0	0	1	1	1	1	4	6	3
AMZ	Amazon	7	6	0	0	1	0	0	1	3	0	0	1	6	1
CAM	Central America/Mexico	6	6	0	2	4	2	1	6	14	6	4	17	42	12
CAR	Small Islands Reg. Caribb.	27	6	0	1	1	0	1	3	6	3	2	9	13	6
Total				**24**	**86**	**245**	**61**	**286**	**498**	**904**	**214**	**763**	**1220**	**1918**	**455**

Table S 8. Multi-sectoral exposed population by IPCC region and indicator scores ≥2.0 and MSR≥5.0 in 2050 under SSP2 (millions of people). For full data see Supplementary data files.

LAB	NAME	IPPC #	Water						Energy				Land				Sectoral			
			w1	w2	w3	w4	w5	w6	e1	e2	e3	e4	l1	l2	l3	l4	Water	Energy	Land	MSR
ALA	Alaska/N.W. Canada	1	0	0	0	0	0	0	0	0	0	0	0	0	0	0	0	0	0	0
WNA	West North America	3	68	45	4	0	26	0	0	23	9	12	7	2	1	0	79	2	2	1
CNA	Central North America	4	35	3	3	0	14	0	0	62	26	16	30	11	0	88	35	27	81	14
ENA	East North America	5	69	0	0	0	31	0	0	59	8	11	24	0	13	105	66	20	76	14
CGI	Canada/Greenl./Iceland	2	0	0	0	0	0	0	0	0	0	0	0	0	0	0	0	0	0	0
NEU	North Europe	11	31	0	0	2	24	0	0	0	0	5	0	0	2	67	26	0	42	0
CEU	Central Europe	12	63	4	0	1	51	0	0	18	0	10	0	1	11	136	59	1	76	0
MED	South Europe/ Mediterr.	13	273	126	58	0	94	14	0	386	95	32	0	206	56	106	272	129	183	108
NAS	North Asia	18	12	8	0	0	22	0	0	0	0	5	0	0	0	1	24	1	1	0
WAS	West Asia	19	185	137	13	2	59	4	0	100	182	39	0	147	7	7	188	172	130	99
CAS	Central Asia	20	201	119	20	2	75	1	97	84	209	14	0	179	12	124	226	198	206	162
TIB	Tibetan Plateau	21	43	27	1	0	11	0	2	54	45	1	2	51	3	53	46	44	59	45
SAS	South Asia	23	1041	213	67	105	307	15	656	2036	1951	84	53	682	51	1827	1033	2028	1858	1108
EAS	East Asia	22	753	113	17	0	170	5	12	388	121	72	0	182	156	1179	711	140	1168	318
SEA	Southeast Asia	24	188	0	7	8	44	0	107	684	627	3	36	3	145	602	182	682	592	408
NAU	North Australia	25	3	0	0	0	2	0	0	2	1	1	0	0	0	1	2	1	1	0
SAU	South Australia/ New Z.	26	20	0	2	0	8	0	0	0	0	13	0	0	0	4	10	5	4	0
EAF	East Africa	16	90	13	16	14	62	8	603	449	127	0	57	33	48	122	98	564	104	65
SAF	Southern Africa	17	51	20	18	1	75	3	258	198	30	0	5	5	2	30	67	218	21	18
SAH	Sahara	14	40	20	1	0	5	2	54	82	86	0	24	5	4	0	41	99	21	22
WAF	West Africa	15	179	4	32	6	116	18	773	849	778	4	31	23	69	422	151	853	319	149
NEB	North-East Brazil	8	19	0	4	0	10	1	0	90	57	8	11	0	9	42	18	61	42	15
SSA	SE South America	10	89	4	1	0	30	0	0	120	9	26	1	5	29	146	76	30	122	31
WSA	W. Coast South America	9	38	19	3	0	4	0	0	25	7	8	0	15	15	5	38	15	22	17
AMZ	Amazon	7	32	1	6	0	7	14	0	51	28	4	18	0	0	20	34	51	11	4
CAM	Central America/Mexico	6	114	27	14	0	29	1	0	184	91	16	63	57	33	177	122	149	170	61
CAR	Small Islands Reg. Caribb.	27	22	0	0	0	3	0	1	40	21	0	0	0	13	26	16	40	23	17
Total			**3659**	**903**	**287**	**141**	**1279**	**86**	**2563**	**5984**	**4508**	**384**	**362**	**1607**	**679**	**5290**	**3620**	**5530**	**5334**	**2676**

Table S 9. Exposed and vulnerable population (income ≤ $10/day) by IPCC region and indicator scores ≥2.0 and MSR≥5.0 in 2050 under SSP2 (millions of people). For full data see Supplementary data files.

LAB	NAME	IPPC #	Water						Energy				Land				Sectoral			
			w1	w2	w3	w4	w5	w6	e1	e2	e3	e4	l1	l2	l3	l4	Water	Energy	Land	MSR
ALA	Alaska/N.W. Canada	1	0	0	0	0	0	0	0	0	0	0	0	0	0	0	0	0	0	0
WNA	West North America	3	0	0	0	0	0	0	0	0	0	0	0	0	0	0	0	0	0	0
CNA	Central North America	4	0	0	0	0	0	0	0	0	0	0	0	0	0	0	0	0	0	0
ENA	East North America	5	0	0	0	0	0	0	0	0	0	0	0	0	0	0	0	0	0	0
CGI	Canada/Greenl./Iceland	2	0	0	0	0	0	0	0	0	0	0	0	0	0	0	0	0	0	0
NEU	North Europe	11	0	0	0	0	0	0	0	0	0	0	0	0	0	0	0	0	0	0
CEU	Central Europe	12	0	0	0	0	0	0	0	0	0	0	0	0	0	0	0	0	0	0
MED	South Europe/ Mediterr.	13	15	7	5	0	4	0	0	19	5	0	0	11	1	5	14	3	10	5
NAS	North Asia	18	0	0	0	0	0	0	0	0	0	0	0	0	0	0	0	0	0	0
WAS	West Asia	19	25	16	3	1	8	1	0	12	24	4	0	22	0	1	24	21	20	11
CAS	Central Asia	20	51	20	9	1	24	0	42	13	46	2	0	32	3	22	54	51	38	30
TIB	Tibetan Plateau	21	5	3	0	0	2	0	1	9	7	0	0	8	1	9	6	7	10	7
SAS	South Asia	23	267	50	18	22	77	4	228	534	505	16	14	184	12	478	261	536	485	282
EAS	East Asia	22	36	6	1	0	9	0	3	24	9	5	0	8	5	64	33	11	62	16
SEA	Southeast Asia	24	11	0	1	1	5	0	37	84	73	0	0	1	10	68	12	84	67	30
NAU	North Australia	25	0	0	0	0	0	0	0	0	0	0	0	0	0	0	0	0	0	0
SAU	South Australia/ New Z.	26	0	0	0	0	0	0	0	0	0	0	0	0	0	0	0	0	0	0
EAF	East Africa	16	39	6	7	9	36	5	349	258	72	0	29	18	28	66	45	330	56	33
SAF	Southern Africa	17	22	7	11	1	42	2	146	120	17	0	2	3	2	19	32	132	13	10
SAH	Sahara	14	13	3	1	0	4	1	31	23	22	0	9	1	2	0	13	32	7	5
WAF	West Africa	15	71	1	17	3	48	11	388	399	360	2	12	12	25	161	68	402	126	49
NEB	North-East Brazil	8	6	0	1	0	3	0	0	26	18	2	3	0	3	12	5	19	12	5
SSA	SE South America	10	10	0	0	0	4	0	0	20	1	3	0	1	2	20	8	4	15	4
WSA	W. Coast South America	9	2	1	0	0	0	0	0	2	0	1	0	1	1	0	2	1	1	1
AMZ	Amazon	7	3	0	1	0	1	1	0	6	4	1	2	0	0	3	3	6	2	1
CAM	Central America/Mexico	6	5	1	0	0	2	0	0	21	10	1	8	1	5	21	5	17	19	6
CAR	Small Islands Reg. Caribb.	27	4	0	0	0	1	0	1	9	4	0	0	0	3	5	3	9	4	3
Total			**585**	**121**	**75**	**38**	**270**	**25**	**1226**	**1579**	**1177**	**37**	**79**	**303**	**103**	**954**	**588**	**1665**	**947**	**498**

6. References

1. Allen, M.R., et al., *Warming caused by cumulative carbon emissions towards the trillionth tonne.* Nature, 2009. **458**(7242): p. 1163-6.
2. IPCC, *Climate change 2013: The Physical Science Basis. Contribution of Working Group I to the Fifth Assessment Report of the Intergovernmental Panel on Climate Change [Stocker, T.F., D. Qin, G.-K. Plattner, M. Tignor, S.K. Allen, J. Boschung, A. Nauels, Y. Xia, V. Bex and P.M. Midgley (eds.)]*, ed. T.F. Stocker, D. Qin, G.-K. Plattner, M. Tignor, S.K. Allen, J. Boschung, A. Nauels, Y. Xia, V. Bex and P.M. Midgley. 2013, Cambridge, United Kingdom and New York, NY, USA: Cambridge University Press.
3. Gillett, N.P., et al., *Constraining the Ratio of Global Warming to Cumulative CO2Emissions Using CMIP5 Simulations*.* Journal of Climate, 2013. **26**(18): p. 6844-6858.
4. Cubasch, U., et al., *Projections of future climate change*. 2001. p. 526-582.
5. Meinshausen, M., S.C. Raper, and T.M. Wigley, *Emulating coupled atmosphere-ocean and carbon cycle models with a simpler model, MAGICC6–Part 1: Model description and calibration.* Atmospheric Chemistry and Physics, 2011. **11**(4): p. 1417-1456.
6. Meinshausen, M., et al., *Greenhouse-gas emission targets for limiting global warming to 2 C.* Nature, 2009. **458**(7242): p. 1158-1162.
7. IIASA. *IAMC AR5 Scenario Database*. 2014; Available from: https://secure.iiasa.ac.at/web-apps/ene/AR5DB/.
8. Raskin, P., et al., *Water futures: Assessment of long-range patterns and problems. Comprehensive assessment of the freshwater resources of the world*. 1997: SEI.
9. Burek, P., et al., *Water Futures and Solution - Fast Track Initiative (Final Report)*. 2016: IIASA, Laxenburg, Austria.
10. Satoh, Y., et al., *Multi-model and multi-scenario assessments of Asian water futures: the Water Futures and Solutions (WFaS) initiative.* Earth's Future, 2017.
11. Wada, Y. and M.F.P. Bierkens, *Sustainability of global water use: past reconstruction and future projections.* Environmental Research Letters, 2014. **9**(10): p. 104003.
12. Wada, Y., D. Wisser, and M.F.P. Bierkens, *Global modeling of withdrawal, allocation and consumptive use of surface water and groundwater resources.* Earth System Dynamics, 2014. **5**(1): p. 15-40.
13. Wanders, N. and Y. Wada, *Human and climate impacts on the 21st century hydrological drought.* Journal of Hydrology, 2015. **526**: p. 208-220.
14. Dankers, R., et al., *First look at changes in flood hazard in the Inter-Sectoral Impact Model Intercomparison Project ensemble.* Proc Natl Acad Sci U S A, 2014. **111**(9): p. 3257-61.
15. Pachauri, S., et al., *Pathways to achieve universal household access to modern energy by 2030.* Environmental Research Letters, 2013. **8**(2): p. 024015.
16. Riahi, K., et al., *Energy pathways for sustainable development.* 2012.
17. Gidden, M.J., et al., *Spatially gridded projections of income and inequality under socioeconomic change.* In review.
18. Bailis, R., et al., *The carbon footprint of traditional woodfuels.* Nature Climate Change, 2015. **5**(3): p. 266-272.
19. Bartos, M., et al., *Impacts of rising air temperatures on electric transmission ampacity and peak electricity load in the United States.* Environmental Research Letters, 2016. **11**(11): p. 114008.
20. Bartos, M.D. and M.V. Chester, *Impacts of climate change on electric power supply in the Western United States.* Nature Climate Change, 2015. **5**(8): p. 748-752.
21. Platts, *World Electric Power Plants Database*, Platts, Editor. 2014, McGraw Hill.
22. Ummel, K., *Carbon Monitoring for Action (CARMA) Database* C.f.G. Development, Editor. 2012: http://www.carma.org/.

23. Raptis, C.E. and S. Pfister, *Global freshwater thermal emissions from steam-electric power plants with once-through cooling systems.* Energy, 2016. **97**: p. 46-57.

24. Rosenzweig, C., et al., *Assessing agricultural risks of climate change in the 21st century in a global gridded crop model intercomparison.* Proc Natl Acad Sci U S A, 2014. **111**(9): p. 3268-73.

25. Havlík, P., et al., *Climate change mitigation through livestock system transitions.* Proceedings of the National Academy of Sciences, 2014. **111**(10): p. 3709-3714.

26. Leclère, D., et al., *Climate change induced transformations of agricultural systems: insights from a global model.* Environmental Research Letters, 2014. **9**(12): p. 124018.

27. Palazzo, A., et al., *Hotspots in land and water resource uses on the way toward achieving the Sustainable Development Goals.* In preparation, 2017.

28. Pastor, A., et al., *Balancing food security and water for the environment under global change.* In review, 2017.

29. Pastor, A.V., et al., *Accounting for environmental flow requirements in global water assessments.* Hydrology and Earth System Sciences, 2014. **18**(12): p. 5041-5059.

30. Fricko, O., et al., *The marker quantification of the Shared Socioeconomic Pathway 2: A middle-of-the-road scenario for the 21st century.* Global Environmental Change, 2017. **42**: p. 251-267.

31. Prestele, R., et al., *Hotspots of uncertainty in land-use and land-cover change projections: a global-scale model comparison.* Global change biology, 2016. **22**(12): p. 3967-3983.

32. Balkovič, J., et al., *Global wheat production potentials and management flexibility under the representative concentration pathways.* Global and Planetary Change, 2014. **122**: p. 107-121.

33. Valin, H., et al., *Agricultural productivity and greenhouse gas emissions: trade-offs or synergies between mitigation and food security?* Environmental Research Letters, 2013. **8**(3): p. 035019.

34. Herrero, M., et al., *African Livestock Futures: Realizing the potential of livestock for food security, poverty reduction and the environment in Sub-Saharan Africa.* 2014.

35. Dunne, J.P., et al., *GFDL's ESM2 Global Coupled Climate–Carbon Earth System Models. Part I: Physical Formulation and Baseline Simulation Characteristics.* Journal of Climate, 2012. **25**(19): p. 6646-6665.

36. Collins, W., et al., *Evaluation of the HadGEM2 model.* Hadley Cent. Tech. Note, 2008. **74**.

37. Dufresne, J.-L., et al., *Climate change projections using the IPSL-CM5 Earth System Model: from CMIP3 to CMIP5.* Climate Dynamics, 2013. **40**(9): p. 2123-2165.

38. Watanabe, S., et al., *MIROC-ESM 2010: Model description and basic results of CMIP5-20c3m experiments.* Geoscientific Model Development, 2011. **4**(4): p. 845.

39. Bentsen, M., et al., *The Norwegian Earth System Model, NorESM1-M – Part 1: Description and basic evaluation of the physical climate.* Geosci. Model Dev., 2013. **6**(3): p. 687-720.

40. Hanasaki, N., et al., *An integrated model for the assessment of global water resources–Part 1: Model description and input meteorological forcing.* Hydrology and Earth System Sciences, 2008. **12**(4): p. 1007-1025.

41. Gerten, D., et al., *Terrestrial vegetation and water balance—hydrological evaluation of a dynamic global vegetation model.* Journal of Hydrology, 2004. **286**(1): p. 249-270.

42. Wada, Y., et al., *Global depletion of groundwater resources.* Geophysical research letters, 2010. **37**(20).

43. Van Beek, L., Y. Wada, and M.F. Bierkens, *Global monthly water stress: 1. Water balance and water availability.* Water Resources Research, 2011. **47**(7).

44. Stacke, T. and S. Hagemann, *Development and evaluation of a global dynamical wetlands extent scheme.* Hydrol. Earth Syst. Sci., 2012. **16**(8): p. 2915-2933.

45. Wisser, D., et al., *Reconstructing 20th century global hydrography: a contribution to the Global Terrestrial Network-Hydrology (GTN-H).* Hydrology and Earth System Sciences, 2010. **14**(1): p. 1-24.

46. Krey, V., et al., *MESSAGE-GLOBIOM 1.0 Documentation*. 2016, International Institute for Applied Systems Analysis (IIASA): Laxenburg, Austria.

47. Riahi, K., et al., *The Shared Socioeconomic Pathways and their Energy, Land Use, and Greenhouse Gas Emissions Implications: An Overview.* Global Environmental Change, 2016.

48. Jones, B. and B.C. O'Neill, *Spatially explicit global population scenarios consistent with the Shared Socioeconomic Pathways.* Environmental Research Letters, 2016. **11**(8): p. 084003.